CHAPTER SIXTEEN

Quality of AM implants in biomedical application

M.J. Mirzaali[a], Nasim Shahriari[b], J. Zhou[a], and A.A. Zadpoor[a]
[a]Department of Biomechanical Engineering, Faculty of Mechanical, Maritime, and Materials Engineering, Delft University of Technology (TU Delft), Delft, the Netherlands
[b]Department of Mechanical Engineering, Brest National School of Engineering, Brest, France

1. Introduction

The expanding and aging population has resulted in a continuous increase in the prevalence of bone tumors and skeletal deformities, and consequently, the world has experienced rapidly increasing demands for bone implants [1]. Bone implants are categorized as the bioimplants that are implanted into the human body, usually for more than 30 days, to be integrated into the human body to fix, support, reproduce, or improve the functions of human tissues [2]. Although bone is known for having self-healing abilities, interventions, such as autografts or allografts, are necessary to restore the bone tissue, if the affected tissue is completely destroyed or degenerated by inflammatory or age-related diseases, and if the bony defect cannot heal itself without surgical intervention. In autograft, a bone taken from the same person's body is used, while in allograft, a bone is taken from a deceased donor. These bone grafts suffer from major limitations, such as the need for multiple operations, donor-site morbidity in the case of autografts, and the risk of infectious diseases from the donor in the case of allografts. Furthermore, allografts are dependent on the availability of the donor and logistics. Therefore, the concept of synthetic bone substitutes has emerged to address these limitations [1,3,4].

An ideal bone substitute offers biocompatibility and mechanical properties close to those of the native bone in order to provide sufficient mechanical support while avoiding stress shielding. It presents a fully interconnected porous structure to serve as a temporary template to aid the diffusion of nutrients and oxygen to allow for bone ingrowth and excretion of the metabolic wastes from the cells. It degrades in the human body over time as the bone regenerates. Developing a porous biomaterial that can fulfill all these requirements has been challenging [1,3].

Quality Analysis of Additively Manufactured Metals
https://doi.org/10.1016/B978-0-323-88664-2.00015-4

Additive manufacturing (AM), also referred to as 3D printing, is an advanced technique used to manufacture objects with complex geometries through sequential addition of material in a layer-by-layer fashion [5,6]. Computer-aided design (CAD) based on patient-specific anatomic data has been utilized in a quest for new developments in the design of bone implants with specific geometry, porosity, pore sizes, and other topological features. Then, the designed implant is manufactured by using one of the AM technologies [3]. The primary principle of all AM technologies is based on slicing a solid model into multiple layers, building the object via layer-by-layer addition of material, and using a heat source (e.g., laser, electron beam, or electric arc) and feedstock (i.e., metal powder or wire) following the sliced model data. This principle makes AM a promising technology for manufacturing objects with structural complexities that are otherwise difficult or impossible to fabricate with conventional manufacturing techniques that require formative (molds) or subtractive (machining) material processing in multiple steps [7].

Recently, a variety of polymers, ceramics, and metals have been developed for bone substitutes. However, not all these biomaterials are suitable for the 3D printing of bone implants [1]. As with anything, there are pros and cons to each of these biomaterial categories. Although polymer-based biomaterials have great flexibility in the design of tailored biodegradation behavior and offer a multitude of routes to biofunctionalization, they have low mechanical properties. Ceramic-based biomaterials are, on the other hand, biodegradable and superiorly osteoconductive. However, the main drawback concerns their brittle nature. Finally, the high mechanical strength and fracture toughness of metals, together with their significant energy absorption capacity, especially those with proper biodegradability, make them the most suitable candidates for load-bearing orthopedic implants [1–3].

Three main types of metal AM techniques have been applied to the fabrication of AM porous implants, namely directed energy deposition (DED), powder bed fusion (PBF), and binder jetting (BJ). DED and PBF are classified as direct metal printing techniques since they do not need post-AM treatments, typically debinding and sintering. In the PBF processes, the energy is delivered to the build area through the source (e.g., laser or electron beam), leading to sintering or melting of powder to build up an object, and as such, they can be further categorized with regard to the heat source into selective laser melting (SLM), selective laser sintering (SLS), and electron beam melting (EBM). The PBF processes are capable of producing complex geometries with internal passages at high resolutions [8]. However, they have a restricted build envelope, and changing the feedstock material is

often complicated, which results in using only single material per part during manufacturing in most AM technology implementations [9]. Nevertheless, in-situ synthesis of materials from powders is possible in certain cases, which means that different feedstock materials with different compositions are fed into the melt pool simultaneously to create objects with desired compositions even at desired locations [10].

SLM is a popular PBF technique to manufacture metallic medical implants since it allows efficient use of raw materials with minimal waste and uses a focused, high power-density laser to melt and fuse metallic powders (Fig. 1A). Moreover, this technique is capable of manufacturing objects with satisfactory geometry accuracy, complex internal features, and passages, and robust mechanical properties that cannot be otherwise produced by traditional manufacturing processes, such as casting or injection molding [1,11,12].

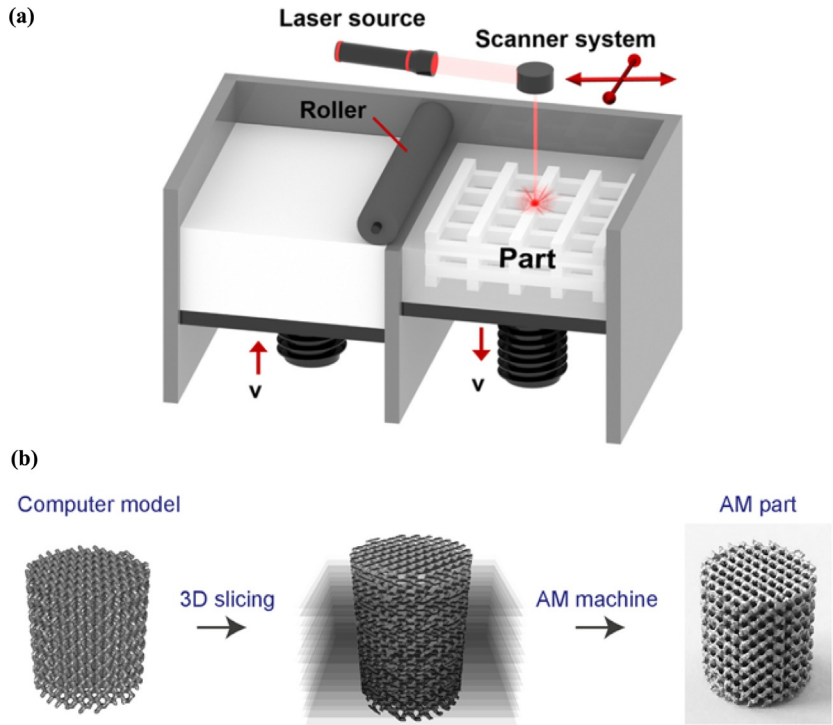

Fig. 1 (A) Schematic illustration of the SLM process. (B) The different steps of AM part manufacturing from a CAD model to the final part. *((A) Reprinted from G. Liu, et al., Additive manufacturing of structural materials, Mater. Sci. Eng. R. Rep. 145 (2021) 100596, https://doi.org/10.1016/j.mser.2020.100596. Copyright (2022), with permission from Elsevier.)*

Powder particle sizes in the SLM process are usually in a range of 10 to 60 μm, and the operation is under an inert atmosphere [13]. Moreover, to better manage the thermal gradients, the powder bed may be heated up to 250°C, which will decrease the adverse effects of thermal stresses [13,14]. The principle of the SLM process is also based on 3D CAD data. In order to process successive layers, slice thickness is required to be in a range of 20 to 100 μm. Due to the diversity of intermediate software packages, in order to facilitate the communication with chosen software, at some point, CAD designs are transformed into the standard tessellation language (STL) format to create the input for the software package installed on the SLM machine. Afterward, the designed AM object is manufactured by setting up the corresponding process parameters and the design of support structures. The aforementioned steps are schematically illustrated in Fig. 1B. In addition, a vector-based approach can be used for printing some objects, particularly the lattice structures that do not need any intermediate STL file and the laser scanning lines are directly related to the geometry of the object that is going to be printed [15].

The quality of SLM products may be measured in different ways, for example, surface roughness, geometrical and dimensional accuracy, physical, chemical, and mechanical properties, depending on the product specifications and intended applications. The overall quality of AM products is first directly related to the quality and characteristics of the raw material loaded into an AM machine, as well as its physical properties such as melting point, evaporation temperature, heat conductivity, absorptivity, and emissivity. In the case of SLM for metals, powder particle morphology, particle sizes, size distribution, impurities, surface roughness, and the possible presence of surface (hydro)oxides all affect the powder packing density, interactions between the powder bed and laser and consequently melt pool dimensions and porosity [16]. In addition, implant design is of critical importance, as it can decide the production success or failure, product quality, and overall costs. Rules of thumb are all known. Guidelines of design for AM must be implemented while making full use of the design freedom and process capacities of AM. The overall quality of AM products is also affected by the build orientation, thermal stresses, possible defects, and microstructure, which are in turn affected by the SLM process parameters often represented by energy density that is a function of laser power, scan speed, powder bad layer thickness, and hatch distance. In the selection of build orientation and SLM process parameters, consideration must be given to the thermal history of the object being built up during the SLM process, which is associated with

the interactions between the powdered material and laser, as well as anisotropic heat conduction along the build direction, in addition to the geometrical features, such as wall thickness, holes, layer marks and overhanging structures. Highly dynamic and complex physical events take place during the SLM process, including melting, possible evaporation, fluid flow, Marangoni flow, heat transfer, phase change, balling, curling, mass transfer, and consolidation. These may lead to residual stresses, delamination, cracking, distortions, porosity, rough surfaces, and thus influence the quality of AM implants. The mechanical properties, particularly dynamic mechanical properties, such as fatigue resistance, are particularly sensitive to residual stresses, porosity, and the nonequilibrium phases formed due to rapid solidification involved in SLM, as well as grain morphology and crystallographic textures. To ensure product quality and reproducibility, it is essential to perform real-time process monitoring and in-process inspection of exact dimensions and develop a closed feedback control system, which is still a huge challenge [17]. In addition to the development of in-situ sensing devices, machine learning to treat and extract crucial information from the captured data has been considered indispensable. To improve the quality of AM products, post-AM processes may be necessary to improve the surface quality, dimensional accuracy, and mechanical properties by means of mechanical or (electro)chemical surface treatments, heat treatments including hot isostatic pressing (HIP), and conventional machining. Considering the distinct AM process features and implant characteristics, the standards commonly used to assess the quality of conventionally fabricated implants may not be suitable and, therefore, need to be either developed or adopted. New material and test standards for AM have been under development, as well as the guidelines on how to adopt existing standards to the unique characteristics of AM implants [18].

In this chapter, we elaborate on the effects of SLM process parameters and postprocessing on the quality of AM products. Particular focus is placed on purpose-designed bone implants, typically with highly porous structures, for biomedical applications. Special attention is given to the mechanical and physical properties of AM bone implants in relation to geometrical design, SLM process parameters, post-AM treatments, and material type.

2. Implant design

Fig. 2 presents the hierarchical structure of human bone at different length scales. An ideal bone substitute should possess mimicking geometries

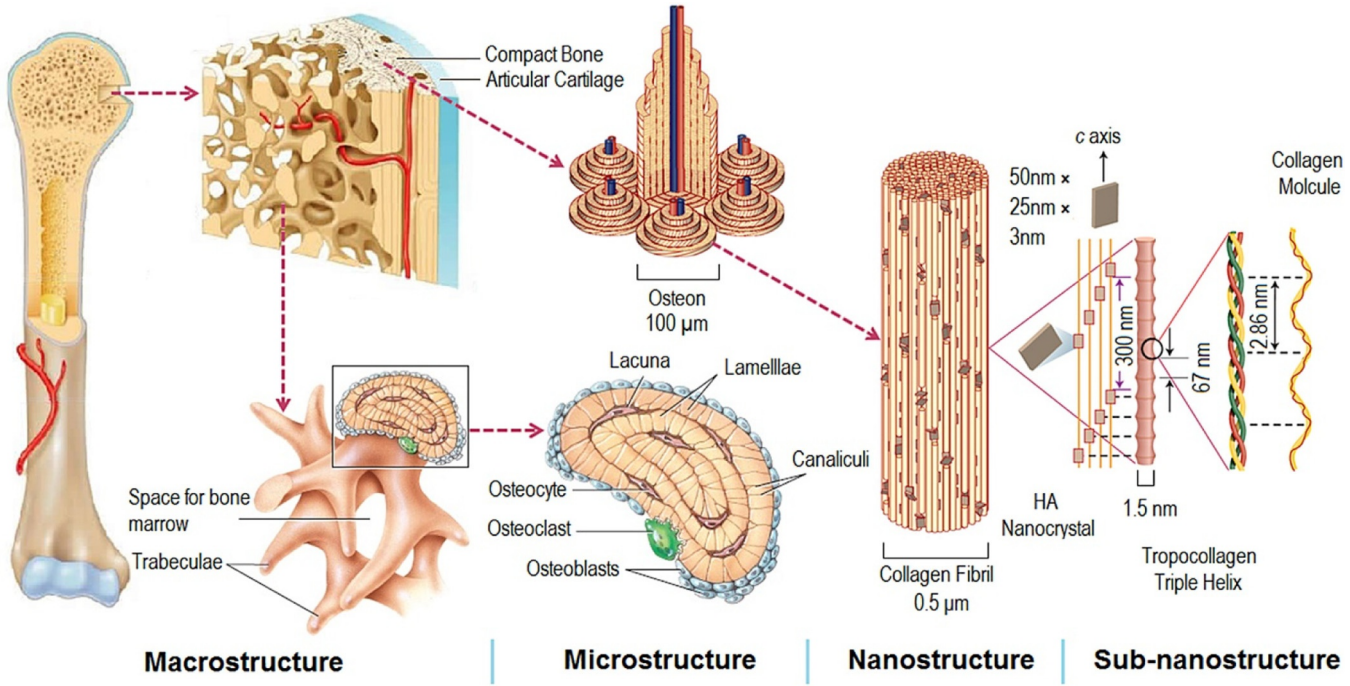

Fig. 2 The hierarchical structure of human bone. *(Reprinted from X. Wang, et al., Topological design and additive manufacturing of porous metals for bone scaffolds and orthopaedic implants: a review, Biomaterials 83 (2016) 127–141, https://doi.org/10.1016/J.BIOMATERIALS.2016.01.012. Copyright (2022), with permission from Elsevier.)*

to better mimic the functionalities and mechanical properties of the human bone. As it can be seen in Fig. 2, the porosity of all types of human bones greatly changes from a compact outer cortical shell toward the spongy inner cancellous tissue [1]. The SLM technique provides the opportunity to manufacture purpose-designed, often patient-specific scaffolds and bioimplants of desired shapes and sizes and even with varying porosities and mechanical strengths. To take full advantage of this opportunity, it is essential to select the most accurate pore shape, pore sizes, and porosity to have an appropriate design for a porous metallic bioimplant. These structural characteristics affect the mechanical properties of porous metallic biomaterials and significantly influence biological performance, such as cell adhesion, proliferation, nutrient transportation, and bone ingrowth [1,6]. Although the SLM process is in general able to offer form-freedom, there are still some design constraints that must be considered, including the maximum/minimum feature size (e.g., wall thickness, edge, and corners), the build direction, the orientation of the lattice with respect to the build direction, and the need for support structures and their removal [19].

2.1 Geometrical design

The effect of the geometrical design of a metallic porous bioimplant can be studied in four domains, namely, mechanical properties, biodegradation behavior, biocompatibility, and bone formation. First, from the mechanical properties point of view, the geometrical design has a strong influence on the porous material, since the yield strength and elastic modulus of a chosen material are dependent on its relative density. Furthermore, the unit cell type should be considered, as it determines both the mechanical properties of the AM porous material and the failure mode of the structure under compression. It has been shown that the geometrical design influences the fatigue behavior of AM porous biodegradable implants as well [1]. Second, the influence of the geometrical design can be studied on the biodegradation behavior of the metallic porous implants due to their location-dependent biodegradation behavior. Space for fluid flow should be considered in implant design to prevent flow stagnation and localized biodegradation. In terms of biocompatibility, the porosity and pore size have significant effects on cell responses and it has been found that they affect the nutrient and waste flow through the scaffolds. Moreover, the geometry can influence cell responses by affecting the biodegradation behavior of the scaffolds. Finally, from the bone formation point of view, the geometrical design,

particularly pore size, is of critical importance, as it can influence the bone ingrowth into the scaffolds [1]. The following sections will more specifically describe the effect of the geometrical design on bioimplants.

2.1.1 Library-based designs

Basically, there are two possible microarchitectures for the lattice structure that may be either regular or irregular. Regular lattices are usually made by repeating one or more types of unit cells in different spatial directions. Beam-based and sheet-based types are the two major unit cell designs. To give an idea, the sheet-based type includes minimal surface designs, such as gyroid, Schwartz P (primitive), and Schwartz D (diamond), usually has reduced quality of the manufactured structure, since it has at least some struts that have a perpendicular orientation to the building direction [1]. In the case of irregular or random lattices, however, there are no specific repeating unit cells. Different categories of lattice structure designs are presented in Fig. 3.

2.1.1.1 Strut-based unit cells

The beam-based designs have been the most studied metallic lattices to date, in which the basic unit cell is created by spatially arranged beam-like structural elements (i.e., struts) (Fig. 3A, B, E, and F). The dimensions and spatial arrangements of struts are used for the determination of the geometry and topology (e.g., connectivity) of repeating unit cells, the morphological parameters of lattice structures (e.g., pore size, relative density), and the overall physical and mechanical properties of the resulting porous materials [23]. Cubic, dodecahedron, and diamond are categorized as the beam-based type that can be further divided from the mechanical point of view into two subcategories of bending-dominated structure that has the ability to absorb a larger amount of energy and stretch-dominated structure that exhibits higher stiffness and yield strength [24,25]. It is however very difficult to achieve pure stretching-dominated or pure bending-dominated lattices, as there is usually a combination of bending and stretching in a unit cell. The Maxwell number can be considered as a criterion in order to determine whether a beam-based unit cell is bending-dominated or stretch-dominated:

$$M = s - 3n + 6 \tag{1}$$

where s is the number of struts and n is the number of joints (i.e., strut intersections).

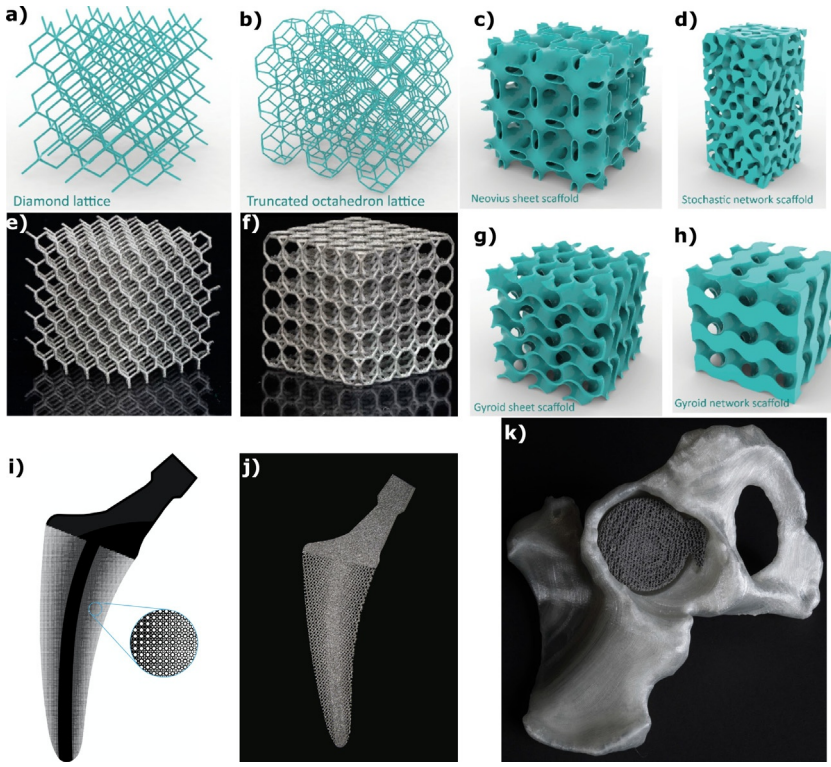

Fig. 3 The beam-based (A, B) and sheet-based (C, D and G, H) CAD designs [20] for the design of microarchitectures of AM lattices. The laser-based PBF process can be used for the manufacture of beam-based structures such as Ti alloys (e.g., Ti6Al4V) (E, F) [21]. Optimization approaches can be applied to the design of the microarchitectures that lead to functionally graded porous structures (I, J). (K) a patient-specific implant fabricated based on computed tomography (CT) images taken from spongy bone [22]. *((I, J) Reprinted from E. Garner, H.M.A. Kolken, C.C.L. Wang, A.A. Zadpoor, J. Wu, Compatibility in microstructural optimization for additive manufacturing, Addit. Manuf. 26 (2019) 65–75, https://doi.org/10.1016/J.ADDMA.2018.12.007. Copyright (2022), with permission from Elsevier.)*

For bending-dominated unit cells, the Maxwell number is $M < 0$, while for stretch-dominated ones, $M \geq 0$ [26].

2.1.1.2 Sheet-based unit cells

Surfaces (shells) are the structural elements constituting sheet-based unit cells and they may be defined using mathematical equations. One specific class of sheet-based unit cells that provide a high level of flexibility in the design of lattice structures [27] are called triply periodic minimal surfaces (TPMS). As TPMS are fully interconnected, they are appropriate scaffold designs to be

used in tissue engineering [27–31]. Moreover, the mean surface curvature of TPMS-based porous structures is zero, which is considered a unique property [32,33]. However, achieving TPMS-based porous structures with high surface quality is complicated. This presents challenges in manufacturing high-quality TPMS geometries with an AM technique and limits the available TPMS designs to those with limited porosity. I-WP, gyroid, Neovius, and diamond are some examples of TPMS geometries (Fig. 3C, G, and H).

2.1.1.3 Nonuniform designs

Nonuniform lattice structures can be created by the changes in both the type and dimensions of unit cells. Functionally graded structures are examples of disordered structures, in which pore sizes vary within the lattices. AM of graded porous structures has in recent years received a lot of attention, since it can prevent stress concentrations by evenly distributing the stresses in the object and also fulfill the contradictory design requirements [31,34]. Despite the challenges in AM of functionally graded lattice structures, especially the ones with highly stochastic or disordered design features, such structures possess several advantages in comparison to the uniform lattice structures. Fig. 3D presents a stochastic network scaffold.

Their first advantage is that they offer a broader range of properties than the ordered ones, which makes it possible to change the properties more smoothly. For instance, mechanical properties such as Poisson's ratio and elastic modulus can be independently and separately tuned due to the rational design of the microstructures [15,25]. Furthermore, thanks to the stochastic nature of random networks, they are less susceptible to the local defects that arise out of the AM process. Finally, it is easier to combine various types of unit cells such as stretch-dominated ones with bending-dominated ones in random network designs, in comparison to ordered ones.

2.1.1.4 Isotropy/anisotropy

The theoretical upper and lower limits of 2D and 3D lattices are defined in terms of elastic modulus (E) and Poisson's ratio (ν) as $0 < \frac{E(\nu)}{3(1-2\nu)} < C_1$, $0 < \frac{E(\nu)}{2(1+\nu)} < C_2$ [35] where C_1 and C_2 are provided by Eqs. (2) and (3), respectively. An increase in the theoretical upper limits of anisotropic lattices can be achieved and such anisotropic structures can be utilized to increase the load transfer efficiency of the lattice structures in specific directions.

$$C_1 = E_b\left(\frac{1}{3(1-2\nu_b)} + \frac{1-\phi}{\frac{(1-2\nu_b)(1+\nu_b)\phi}{(1-\nu_b)} - 3(1-2\nu_b)}\right), \tag{2}$$

$$C_2 = E_b\left(\frac{1}{2(1+\nu_b)} + \frac{1-\phi}{\frac{4(4-5\nu_b)(1+\nu_b)\phi}{15(1-\nu_b)} - 2(1+\nu_b)}\right) \tag{3}$$

where E_b and ν_b are, respectively, the elastic modulus and Poisson's ratio of the base material, and ϕ is defined as the volume fraction of the lattice structure [36].

2.1.2 Topology optimization

The optimum material distribution within a design space is obtained by applying a powerful approach called topology optimization that makes use of computational and mathematical models to design the optimized arrangements of the microstructure of porous structures to obtain desired and optimal properties while satisfying certain conditions [37]. One of the developed optimization approaches is called the "inversive homogenization" technique, which allows the finding of a spatial arrangement of unit cells in 3D space to provide unusual properties, such as negative thermal expansion coefficient and negative refraction index [37–39]. The conventional manufacturing process is often too complex and costly to manufacture topologically optimized structures, while AM can address these problems by its "complexity-for-free" characteristic. Although AM can realize a wide range of geometries, it cannot print long overhangs without internal support structures.

AM lattices can be designed by using a variety of objective functions, such as maximizing the specific stiffness (stiffness to mass ratio), which may lead to the lattices with trabecular bone-like microarchitectures [40–42]. Bone substitutes are designed by using optimization models based on bone tissue adaptation processes (Fig. 3I and J) [43–46]. Furthermore, strain energy can be utilized as some other objective functions. To optimize multiple objective functions simultaneously, the algorithms of multiphysics topology optimization can be used. To this end, the maximum bulk modulus or elastic modulus can, for instance, be merged with specific values of permeability [47–49]. Optimization techniques for finding the optimized topology of lattice structures with multifunctional properties include evolutionary structural optimization (ESO) [50], solid isotropic material with penalization (SIMP) [51,52], bi-directional evolutionary structural

optimization (BESO) [53,54], and level-set algorithms [54]. TOSCA, Pareto works, PLATO [55], and freely available codes [55] are some of the various optimization tools that can be utilized for design purposes. In this connection, it can be mentioned that the integration of specific requirements of the AM processes into topology optimization algorithms is an active research field, and optimizing the arrangements of support materials for successful AM processes by algorithms is an example of such integration (e.g., see [56,57]).

2.1.3 Patient-specific design

Diversity in the size, shape, and geometry of an individual's bones has made it essential to consider custom-made designs for patient-specific AM biomaterials and orthopedic implants, since no single design matches all the requirements for each application [58–60] (Fig. 3K). In patient-specific designs, the CAD model of the implant is based on the images obtained mostly from magnetic resonance imaging (MRI) or computed tomography (CT) [61].

2.1.4 Bio-inspired design

Bio-inspired design is an approach to designing lattice structures based on natural cellular materials like bone [62]. Several key design elements have to be taken into consideration in the design of such structures and they can be translated into bio-inspired porous materials. Orthopedic implants are the major applications of bio-inspired designs since it is essential to perform surgical procedures for facilitating bone healing in critical defects [63]. The bio-inspired designs act as alternatives to allograft and autograft implants to address the challenges of using these biological materials, e.g., limited availability and medical issues, as mentioned above [64].

The geometry of the biomimetic lattice structures that are expected to help tissue reconstruction can be created by using CT, or MRI images [65,66]. Patient-specific designs (Fig. 3K) are also considered bio-inspired designs inasmuch, as their geometry and dimensions should match the anatomy of the patient. In addition, cancellous (or trabecular) bone is an example of the bio-inspired cellular material that is made of hydroxyapatite crystals and collagen molecules formed at several hierarchical levels, and actually, it is a porous biological material [67]. The volumetric components (i.e., connecting rods and plates) of trabeculae constitute the cellular structure of the cancellous bone and since the porosity is spatially distributed in the structure, the trabecular bone can be seen as a functionally graded material [67].

2.1.5 Metabiomaterials

Thanks to the advent of AM, the developments of new materials in materials science have occurred in the domain of applied physics, in addition to applied chemistry, and the novelty in materials properties has been achieved by the "rational design" process. To establish the design-property relationships in rational design, theoretical considerations, analytical solutions, and computational modeling are all needed in the design of material with specific properties at a macro scale by estimating the microscale spatial distribution and topological design. Concerning the desired properties, metamaterials are categorized into three groups of mechanical metamaterials, acoustic metamaterials, or metabiomaterials that are shown in Fig. 4. This section concerns the design of metabiomaterials [68].

In comparison with traditional composites, metamaterials refer to engineered (composite) materials whose properties could be different from those of the constituting phases such as negative Poison's ratio, and negative stiffness for mechanical metamaterials and acoustic cloaking for acoustic metamaterials, which are not usual in natural materials. Moreover, in the topological design of metamaterials, "voids" are considered as the second phase constituent, when the metamaterial consists of one type of material [42,68–70].

Metabiomaterials are the third type of metamaterials, whose biomedical application is of interest. They are principally multiphysics metamaterials and possess distinct topological, mechanical, and biological properties. Moreover, metabiomaterials have two additional advantages. First, they can be utilized in surface bio-functionalization applications since they have a totally interconnected surface area, which is much larger than the solid counterpart by several orders of magnitude. Second, they are capable of accommodating drug delivery vehicles through their fully interconnected pore space [32,33,71]. Recently, the bone-mimicking properties of metabiomaterials together with their potentially superior properties, which have been developed by rational design and through topological design, have made them capable of being used as either bone substitutes or components of orthopedic implants for bone tissue regeneration and osseointegration purposes and extending the implant's life [68,72].

It is of great importance to make a distinction between the diverse types of mechanical properties such as elastic modulus, Poisson's ratio, and yield strength. These properties will be discussed separately. In terms of elastic modulus, the metabiomaterial should not have an elastic modulus greater than that of the natural bone that is intended to be replaced, since it has been

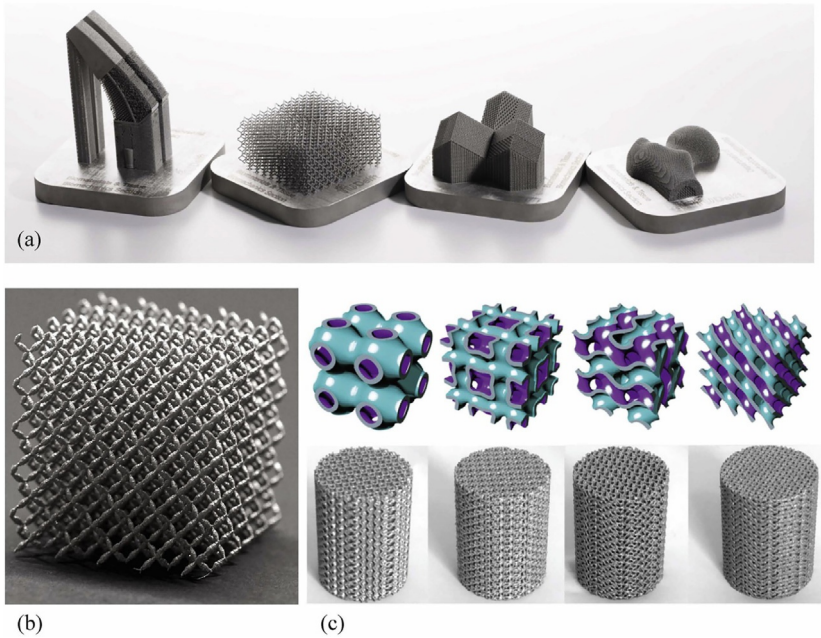

Fig. 4 SLM Ti-6Al-4V samples of (A) various porous metabiomaterials and implants with different functionalities for different applications. (B) Penta-mode mechanical metamaterials known as meta fluids. (C) Triply periodic surfaces based on sheet-based lattice structures. *((A) Reprinted from A.A. Zadpoor, Mechanical performance of additively manufactured meta-biomaterials, Acta Biomater. 85 (2019) 41–59, https://doi.org/10.1016/j.actbio.2018.12.038. Copyright (2022), with permission from Elsevier. (B) Reprinted from R. Hedayati, A.M. Leeflang, A.A. Zadpoor, Additively manufactured metallic pentamode meta-materials, Appl. Phys. Lett. 110(9) (2017) 091905, https://doi.org/10.1063/1.4977561. Copyright (2022) with permission from AIP. (C) Reprinted from F.S.L. Bobbert, et al., Additively manufactured metallic porous biomaterials based on minimal surfaces: a unique combination of topological, mechanical, and mass transport properties, Acta Biomater. 53 (2017) 572–584, https://doi.org/10.1016/j.actbio.2017.02.024. Copyright (2022), with permission from Elsevier.)*

established that mechanical loading increases bone growth and remodeling. The absence of loading on the surrounding bone will take place if the used bioimplant is too stiff and this causes bone resorption and inhibits bone regeneration. This is called the stress-shielding phenomenon. However, the yield strength of the biomaterial is independent of the native bone and a metabiomaterial can be considered ideal if it has a yield strength as high as possible while its elastic modulus is close to that of the native bone [68]. Since accurate measurement of elastic modulus is complicated in

comparison with the yield strength measurements and as there is a strong correlation between these two properties in the most conventional materials, the (yield or ultimate) strength is often measured instead of the elastic modulus. However, in some classes of metabiomaterials, the expected correlations between yield strength and elastic modulus may not be valid, as there are no a priori relationships between them and the strength cannot be used as a surrogate measurement of elastic modulus. The reason is that the mechanical properties of the metabiomaterials are structure-dependent measurements rather than intrinsic properties and they measure the macroscale behavior of an architected material when the length scale of the structure is much larger than the small-scale designed repetitive unit cell's dimensions [68].

3. Effects of process parameters on the quality of AM implants

Although the SLM process is able to manufacture implants with complex geometries, the success of the process and the quality of the final printed implant are dependent on the chosen process parameters. The quality, quality consistency, and reliability of AM materials are often achieved by adjusting and controlling the process parameters. Three main criteria of successful printing are as follows. First, the manufactured defectless AM implant must have the same material composition as the parent counterpart. Second, the geometry of the printed implant has to be the same as the CAD design. Finally, the printed implant should meet certain requirements in quality with respect to surface roughness, microstructure, and mechanical properties. To meet these criteria, the selection of SLM process parameters is of paramount importance, as it can result in manufactured objects with similar or even better mechanical properties than the conventionally manufactured ones [73].

Some of the effective SLM process parameters are laser energy power, laser line spacing, laser diameter, laser scanning speed, scanning strategy, and build-plate preheat temperature [11,74]. To solve multivariable optimization problems, various process maps have been developed to help with the identification of optimum process parameters. Although the proposed maps can indeed help with the proper selection of the SLM process parameters, such as laser beam power and scan speed, it is often a money- and time-consuming process to find them. Moreover, they are likely both machine- and design-specific [74–77].

3.1 Morphological properties and geometrical fidelity

To consider an AM process a successful one, the printed implant must have the same geometry as the CAD design (geometrical fidelity). In addition, the mechanical properties of AM lattices, such as fatigue resistance, are strongly dependent on morphological designs. It is therefore of great importance to quantify the deviations of the as-built implants from the as-designed implants [78,79]. The extent of morphological deviations is largely determined by the geometry complexity and the process parameters. Local variations in strut thickness, waviness, and node sizes [80] can be measured by using a variety of nondestructive methods, including scanning electron microscopy (SEM), microcomputed tomography (μ-CT), and optical and confocal microscopies (Fig. 5A–E). It has been found that the objects fabricated by the SLM process have a more accurate geometry than that by the DED process [81]. Strut cross-sectional irregularities (Fig. 5A) and microdefects resulting from the unintended and accidental fusion of powder particles (Fig. 5B and C) are the two kinds of defects generated in the printed implants during the SLM process, which would result in micro porosity at the microstructure of porous materials [40].

3.2 Surface quality

The surface quality of AM products is commonly measured by surface roughness, regardless of the AM technique used. Different AM techniques may result in a broad range of surface roughness values. For some biomedical applications, the high surface roughness of AM implants or scaffolds is regarded as an advantage as a rough surface tends to encourage cell attachment [23]. An optical profilometer and SEM can be used to measure the surface roughness and analyze the surface morphology, respectively [82]. In addition, the heights of peaks and valleys at different locations of a rough surface of an AM object are quantified using some empirical equations [82]. The achievable minimum surface roughness of SLM parts is typically 10 μm, unless micro-SLM is applied [83]. In many cases, mechanical and (electro)chemical posttreatment processes are needed to improve the surface quality of AM objects, including machining, grinding, polishing, shot-peening, and chemical etching [84,85].

In the SLM process, the layer thickness is typically 30 μm. It is thinner, as compared to the layer thickness typically used in the EBM process (70 μm). Moreover, the scanning speed is slower and fine powders are used in the SLM process. Therefore, the products manufactured by the SLM process

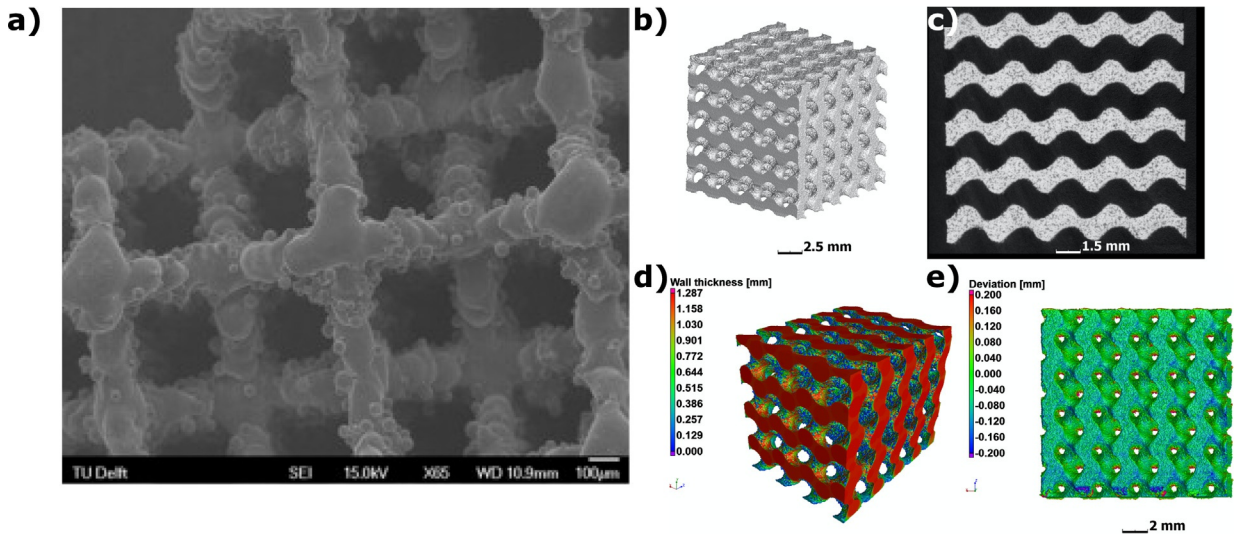

Fig. 5 (A) The geometrical irregularities caused by the inappropriate selection of SLM process parameters. (B, C) The microporosity in the struts of a lattice structure, (D, E) nondestructive imaging techniques for quantifying the morphological variations. *((A) Reprinted from G. Campoli, M.S. Borleffs, S. Amin Yavari, R. Wauthle, H. Weinans, A.A. Zadpoor, Mechanical properties of open-cell metallic biomaterials manufactured using additive manufacturing, Mater. Des. 49 (2013) 957–965, https://doi.org/10.1016/j.matdes.2013.01.071. Copyright (2022), with permission from Elsevier. (B–E) are reprinted from A. du Plessis, S.M.J. Razavi, F. Berto, The effects of microporosity in struts of gyroid lattice structures produced by laser powder bed fusion, Mater. Des. 194 (2020) 108899, https://doi.org/10.1016/j.matdes.2020.108899. Copyright (2022), with permission from Elsevier.)*

have a quite smooth surface in comparison to the other AM techniques such as EBM or DED. For example, a fine particle size of $<20\,\mu m$ in the SLM process corresponded to a thinner layer and a product with a smoother surface finish, although the production rate would be lower [12,86,87].

Furthermore, powder characteristics can have an effect on surface roughness. For example, irregular powder particles with coarser surface textures would result in high surface roughness. The powders manufactured by the water atomization process would lead to AM products with high surface roughness in comparison to the ones produced by gas atomization [88]. Moreover, the quality of the surface can also be affected by the quality of re-used powders [89].

The features of the SLM process that can affect the surface roughness of AM products are the balling phenomenon and defect formation. For example, unmolten powder particles resulting from an inappropriate selection of laser power energy and thus insufficient energy delivery to powder particles would stick to the surfaces of AM products and increase surface roughness [90–92].

The build rate is one of the process parameters that decide the surface quality. As the surface quality and resolution have a contradictory relationship with the build rate, the objects manufactured at a high build rate tend to be subjected to post-AM treatments. It is worth noting that the mechanical properties, particularly the fatigue behavior of AM products, vary with the surface quality, as surface irregularities tend to act as stress concentration sites and lead to crack initiation. This makes it essential to apply surface treatments, such as mechanical or (electro)chemical polishing or machining, to enhance the surface quality of AM products [93] in cases where fatigue resistance is of particular importance, in addition to surface appearance and low friction.

3.3 Microstructures

One of the most important factors that determine the mechanical and functional properties of a 3D printed object is its microstructure. It is essential to select proper SLM process parameters in order to manufacture AM materials without any defects or unintended micropores. The developments of SLM process windows can lead to manufacturing lattice structures with a minimum number of defects, mostly micropores which can be measured by defining the relative density (ρ). The relative density of a lattice structure is one of the essential parameters to define its mechanical and physical

properties and it is described as the portion of solid constituents in the nominal volume of the porous body. Archimedes' principle and microscopic or μCT analysis are the commonly used methods to measure the relative density of porous structures. The measured values are often compared with CAD design values to determine the deviations. The mismatch may be caused by the defects and irregularities that have been generated in AM lattice structures [94,95].

For instance, the density of the energy delivered to and absorbed in the melting material would strongly influence the generation of micropores by having a direct effect on the gas/flow interactions and evolution of temperature [96–98]. As a general principle, a too low power density would result in insufficient melting and it would increase microporosity. On the contrary, a too high power density might have some adverse effects on the melt pool by keyhole pore formation that might cause the formation of a turbulent melt pool, splash of the molten material, evaporation of alloying elements, and formation of gas bubbles by entrapping inert gas as the material resolidifies [99].

Insufficient melting by increasing the hatch spacing or the thickness of the powder layer can on the one hand increase the surface roughness of struts and deteriorate the fatigue resistance and other mechanical properties of porous biomaterials. On the other hand, it can cause the formation of unwanted micropores, especially in thick struts, which would affect the functionality and mechanical properties of the printed lattice structure [99].

The cooling rate is another factor that may lead to either a finer or a coarser microstructure and can be adjusted by the power and velocity of the energy source and the substrate preheating temperature. For example, laser PBF processing of Ti-6Al-4V can result in an $\alpha + \beta$ lamellar microstructure [76,100,101]. Furthermore, various AM microstructures can be obtained from various solidification mechanisms. For instance, a metastable phase can be formed due to rapid solidification involved in SLM, resulting in AM products with higher mechanical strengths. Moreover, partially molten particles can act as a preferred zone of nucleation and equiaxed grains can heterogeneously nucleate on them, and/or parent grains can undergo epitaxial growth [94,102].

In addition, the homogeneity and microstructural banding of the SLM materials are affected by the thermal history during the SLM process that results from the layer-by-layer nature of the AM process. The repeated thermal cycles cause various liquid-solid transformations in each deposition layer and result in microstructural banding. Additionally, the microstructures with

preferred directionality (anisotropy) can be obtained from the temperature gradient that results from directional heat flow [103–108].

The two strongly influential SLM process parameters that actually control the size and morphology of the microstructure are the scanning speed and laser power. To give a rough idea about their influences, it can be mentioned that a higher scanning speed with a lower laser power creates a finer microstructure. By contrast, a coarser microstructure is obtained from a lower scanning speed combined with higher laser power. However, the final microstructure can also be controlled through applying postprocessing techniques, such as HIP and heat treatment [109,110].

3.4 Chemical composition

The mechanical properties of AM lattice structures are controlled by the phase transformation occurring during the AM process and the as-built microstructure of the AM product that is first determined by the chemical composition of the material in the powder bed. Therefore, adding or omitting any alloying elements, which might be intentional or due to environmental factors, such as humidity or atmospheric conditions, such as the oxygen level, can strongly affect the outcome. For instance, a large amount of oxygen in the atmosphere would cause oxidation and the creation of an oxide layer or inclusions in the product during the AM process, which would cause decreases in mechanical properties [111]. As another example, during compressive testing, some of the Ti-based cellular structures show brittle behavior with no plateau region in their stress-strain curves, if large amounts of interstitial atoms, such as O, N, and C, are entrapped in the crystal structure. Moreover, alloying Ti with Nb or V would enhance the β phase stability, and the β to ά (martensite) transformation would be restricted so that the as-built lattice structure might have better ductility [112,113].

It is of great importance to control the AM process parameters, particularly the energy input and temperatures that can accelerate the chemical degradation and oxidation of AM products, and to use an inert atmosphere in order to minimize the amounts of impurities. The effect of pore-inducing agents on the chemical composition of raw powders in the design process of porous materials should be considered, since it may cause an increase in pore formation during the AM process [114]. In addition, recycling of the powders from previous SLM runs may become a source of different chemical compositions and powder characteristics in one specific powder material and thus affect the mechanical properties of AM products and reproducibility [112,113].

3.5 In situ residual stress relief

The occurrence of local and global thermal gradients during the 3D printing process, due to rapid heating and cooling involved in the SLM process, leads to the development of residual stresses in the lattice structure of AM implants. In other words, the thermal history of AM materials largely determines the magnitude of residual stress. Residual stress may have diverse effects on the mechanical performance and geometrical and dimensional accuracy of AM products (Fig. 6A) [115].

The type and level of residual stresses in AM materials are mostly defined by the SLM process parameters applied, typically the laser power, hatch distance, layer thickness, scanning strategy, and scanning speed. Furthermore, the level of residual stress is influenced by the physical and mechanical properties of the powdered material itself, such as the thermal expansion coefficient, thermal conductivity, Young's modulus, and yield stress [116,117].

In-situ residual stress relief may be applied to minimize residual stresses by optimizing the SLM process parameters, such as preheating the substrate or the previously deposited layer, using proper scanning strategy, and placement of supports at appropriate places that leads to minimized distortions of AM implants [75,118,119]. Preheating the substrate is particularly effective in reducing the temperature gradients and cooling rates in the metal and thus the magnitudes of shrinkage stresses. This is confirmed by the observation that the implants fabricated by the SLM process typically have higher magnitudes of residual stresses, as compared to those of EBM that includes substantial substrate preheating in the manufacturing process [9].

4. Effects of postprocessing on the quality of AM implants

Porous materials manufactured with the SLM process may include defects such as microporosity and lack of fusion (LOF), and powder particles may adhere to their struts. Various post-AM processes, such as heat-treatments at a high temperature combined with pressure, can significantly change the mechanical properties, biodegradation behavior, biocompatibility, and bone formational behavior of AM materials by improving the microstructure, relative density, and balance in mechanical properties. Although these processes can result in achieving new functionalities and reducing residual stresses, they may affect the cost-effectiveness of the AM fabrication route [120].

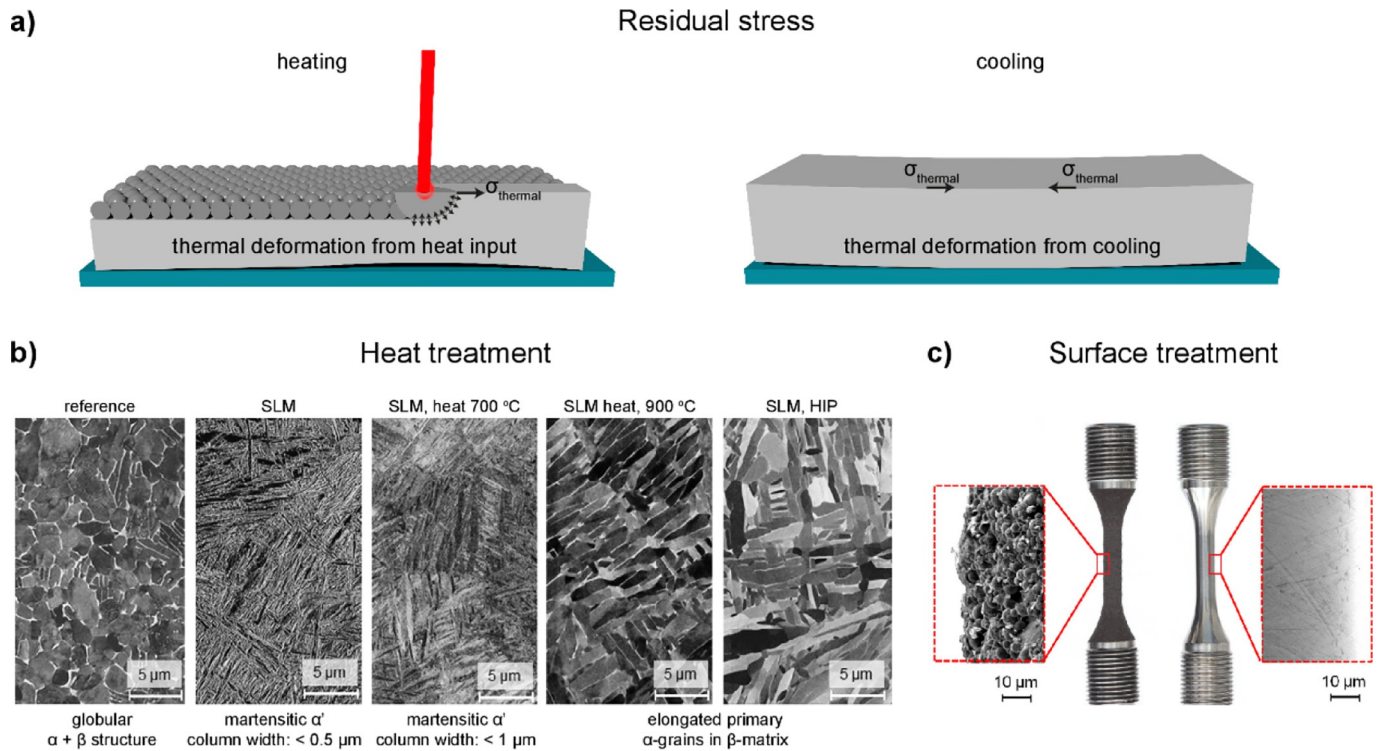

Fig. 6 The residual stress and the effect of post-AM treatment, (A) the way in which the residual stresses created, (B) SEM micrographs showing the microstructures of SLM Ti6Al4V. From left to right: globular "reference," lamellar structure of the SLM Ti-6Al-4V alloy and the effects of thermomechanical treatment on the microstructure of SLM specimens [30], (C) surface treatment applied to the tensile test specimen. The left one is the as-built and the right one is the as-machined. *((B–E) are reprinted from G. Kasperovich, J. Hausmann, Improvement of fatigue resistance and ductility of TiAl6V4 processed by selective laser melting, J. Mater. Process. Technol. 220 (2015) 202–214, https://doi.org/10.1016/j.jmatprotec.2015.01.025. Copyright (2022), with permission from Elsevier.)*

4.1 Heat treatments

The microstructures of SLM products change by applying heat-treatment processes through influencing their grain sizes and precipitates [119,121] (Fig. 6B). The annealing process is effective in removing residual stresses developed during the SLM process through intensified atomic diffusion at elevated temperatures. Furthermore, the duration of the heat-treatment process plays a role in determining the extent of microstructural changes of AM products [119]. However, the same type of heat treatment can have diverse effects on different materials. For example, for SLM WE43 magnesium alloy scaffolds, annealing was found to decrease their compressive strength, while for SLM iron scaffolds a vacuum annealing process increased their yield strength by causing grain refinement [1]. Moreover, raising the heat treatment temperature for Ti6Al4V parts to above the ß transus temperature would lead to coarsening the prior β-grains and dissolving the α phase and thus reducing yield stress [122].

The global heat-treatment may not be an appropriate process for AM implants since it can affect their geometrical accuracy and mechanical properties. To address this challenge and since the residual stress is spatially distributed in the AM object, local heat treatment can be used for these implants. For this purpose, computational modeling can help with the determination of the exact place of residual stress in AM implants.

4.2 Surface treatments

Porous materials manufactured by using the PBF processes often have powder particles adhered to their struts and therefore surface treatments are essential for smoothening the surfaces of these AM materials [123]. There are a variety of surface treatment processes that can be categorized into mechanical (e.g., machining, and polishing (Fig. 6C)) and chemical (e.g., etching) processes [85,124]. Because of the change of surface characteristics, the bioactivity, biocompatibility, corrosion resistance, and fatigue strength of AM porous biomaterials can be enhanced. Sandblasting is one of the surface treatments based on the physical erosion by abrasive materials. With this surface treatment, excess powder particles that are adhered to the surfaces of struts can be removed and a nanocrystalline thin film that covers the outer region of them is formed. In addition, compressive residual stresses are introduced to the superficial region of struts. Although this process can increase the endurance limit of AM lattices, abrasive materials cannot reach the inner layers and internal struts of the lattice structures [123].

4.3 Hot isostatic pressing (HIP)

HIP is a process often used to close up the imperfections and micropores that have been generated inside AM products during the manufacturing process. During the HIP process, high pressure and high temperature are applied simultaneously to the AM products, leading to increases in fatigue life and quasistatic mechanical properties of AM biomaterials [125–128]. However, the degree of anisotropy may decrease in metallic lattices, and the yield strength may decrease due to the rise in temperature and a certain level of annealing during HIP [129].

The effect of the HIP treatment on the fatigue behavior of AM lattice structures is still contentious. In some studies on Ti-6Al-4V [130] and CoCr alloy [131] lattice structures, no enhancements in fatigue behavior have been reported. The reason can be that the microstructural defects on the top surfaces, such as strut thickness variations and strut waviness, cannot be fixed by the HIP treatments and as a result, such defects still act as preferred crack initiation zones [130]. Fig. 6B presents the effect of the HIP process at 900°C and 100 MPa on the microstructure of the AM Ti-6Al-4V. Due to HIP, the martensitic structure drastically changed into elongated α grains embedded in α/β-phase grain boundaries, in addition to a reduction in microporosity, and tensile ductility and fatigue strength were improved at the sacrifice of yield strength, as reported by other researchers [129,132,133].

4.4 Chemical treatments/biofunctionalization/coating

Chemical etching is a surface treatment method that is used for modifying surface roughness. The etchant is able to reach internal struts and thus this process can address the limitation of sandblasting. However, it may not always have a positive effect on the fatigue performance of lattice structures, which appear to be alloy-dependent [128]. Chemical surface treatment can be categorized into two subcategories: light chemical surface treatment and chemical surface treatment to induce specific (bio-) functionalization (Fig. 7A–G). By applying light chemical surface treatments, unmolten powder particles are eliminated from strut surfaces. As the fatigue performance of a porous material is governed by surface roughness, residual stresses, manufacturing defects, microstructure, and loading conditions, applying some chemical surface treatments for the sake of bio-functionalization may also improve the fatigue properties of porous biomaterials [131]. A combination of surface treatments (e.g., chemical etching and sandblasting) with HIP can surely improve the fatigue life of AM lattices [126]. In addition

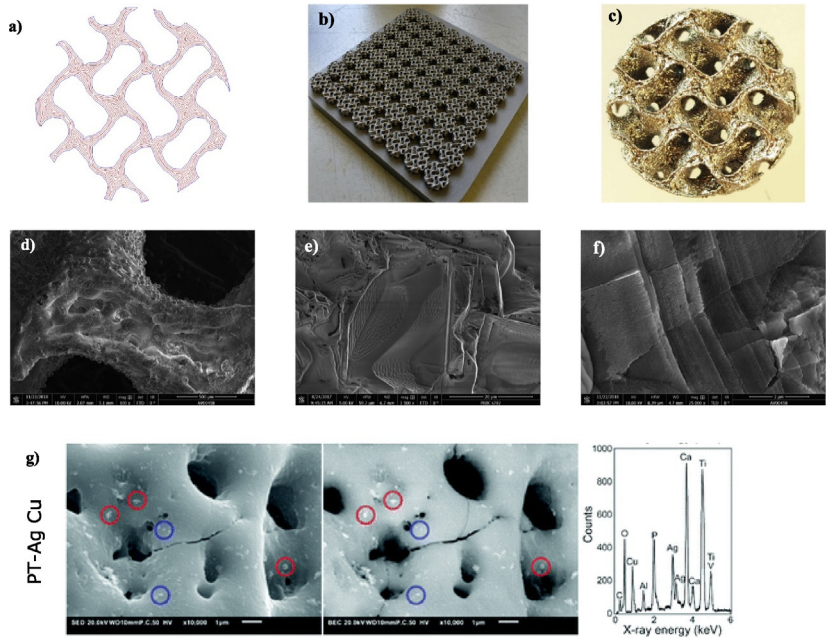

Fig. 7 (A–F) Various post-AM treatments applied to AM biomaterials [134], and (G) addition of specific particles such as silver and copper nanoparticles to activate the self-defending ability of lattice structures [135].

to improving fatigue performance, surface modification and surface coating can enhance the bioactivity of AM porous biomaterials [126].

Surface bio-functionalization processes, including chemical and electrochemical surface treatments and coatings, improve the tissue regeneration performance of AM metabiomaterials and can put a stop to implant-associated infections. However, in some cases, the erosion and roughening of struts of AM lattices for the sake of bio-functionalization may have adverse effects on the mechanical properties and decrease them [23,136–138].

Sol-gel is one of the surface coating methods known for being a low-cost process and able to create coating layers with uniform and homogenized microstructures along with bioactive properties. During this process, an oxide layer is applied to the surface of an AM porous biomaterial at a low temperature [139,140]. In addition, alkali treatment, acid etching and anodizing are some other surface treatments that are based on the reaction between the surface of AM porous biomaterials and a corrosive chemical solution. However, the alkali-acid surface treatments and plasma electrolytic oxidation have shown no effect on the fatigue life of AM lattices [141–146].

5. Materials

A wide range of biomaterials has been developed. However, not all of them are appropriate for 3D printing to fabricate bioimplants. Bioimplants should be prepared with materials that have basic properties, such as low toxicity and good biocompatibility. Moreover, the adhesion of cells to the surfaces of biomaterials and cell proliferation should be easy. It is also important for bioimplants to possess an appropriate wear resistance and biodegradability, but not to release toxic elements in the human body due to wear or biodegradation. In addition, due to the variety of the locations in the human body where these bioimplants can be used (e.g., bone, cartilage, and joints), the application environment should be taken into consideration to meet the specific requirements [2,4].

The chemical and physical properties of biomaterials together with their mechanical properties have to be considered in material selection for 3D printing to fabricate implants, particularly for load-bearing implants. Metals have been found to be the most suited biomaterials for load-bearing implants and are introduced in the following [2].

5.1 Metals and alloys

SLM is usually used for the 3D printing of implants made of metals or alloys. For metallic porous implants, material type and alloying can affect the mechanical properties of the bioimplant and the biological responses of cells to the bioimplant. This section reviews some categories of metallic materials that are appropriate candidates for the fabrication of metallic lattices by using the SLM process [1,2].

5.1.1 Biomedical and biodegradable metals

The three basic criteria that any metal that is going to be used in biomedical applications should have, are good biocompatibility, corrosion resistance, and mechanical properties. It is however important to note that for a special group of metallic biomaterials, their corrosion in physiological environments is positively utilized to allow their biodegradation over time. Such biomaterials can be used in temporary bioimplants to support the healing process and assist in the regeneration of native tissue. This special group of biomaterials are called biodegradable materials. So far, the common metals

and alloys that have been used for the 3D printing of biodegradable and non-biodegradable implants include titanium and Ti-based alloys [147,148], stainless steel, Co-based alloys, Mg and its alloys, Zn-based alloys, Zr, Nb, Ta, and iron and its alloys.

5.1.1.1 Titanium and Ti-based alloys

High corrosion resistance, low elastic modulus, and good biocompatibility are the main reasons for the use of Ti alloys as biomaterials. Ti-6Al-4V [149], Ti-6Al-7Nb, and Ti-5Al-2.5Fe are the Ti-base alloys that have been used to fabricate bioimplants. Ti-6Al-4V alloy implants have, for example, been fabricated as mandibular, clavicular, dental, and hip implants, since the alloy has high specific strength (strength to density ratio), excellent corrosion resistance, and appropriate fatigue properties [150,151]. However, the release of Al and V ions from these implants can cause side effects, including osteomalacia, Alzheimer's disease, and other neurological disorders. To solve this problem, V-free alloys, such as Ti-5Al-2.5Fe and Ti-6Al-7Nb, have been developed for femoral prostheses, and V- and Al-free alloys, such as Ti-2Mo-0.5Fe, Ti-3Mo-0.5Fe, and Ti-4.7Mo-4.5Fe, have shown better biocompatibility than Ti-6Al-4V [152]. For certain applications, surface modification and the addition of refractory metal elements, such as Nb, are required to achieve better wear resistance [2,153]. In addition to SLM of Ti-based alloys, SLM of porous pure Ti has become attractive, as the material does not contain any possibly hazardous alloying elements and it is very biocompatible. Although it has a lower specific strength, compared to the Ti alloys, particularly Ti-6Al-4V, it is a biomaterial suitable for many nonload-bearing or mild-load-bearing biomedical applications, such as cranio- and maxillo-facial implants to take advantage of its excellent in vivo performance, lower cost, higher ductility, and enhanced normalized fatigue resistance [153–159].

5.1.1.2 Stainless steel (SS)

Stainless steel is one of the candidates of AM bioimplants for its biocompatibility, low cost, and ease of fabrication by laser-based PBF processes. One of the main considerations in AM of SS is the cooling rate that affects the final microstructure and results in the presence or absence of the martensitic phase in SS. For instance, in the case of comparing SLM and conventionally manufactured 316L SS, the SLM 316L SS has been found to have a refined microstructure by prohibiting the growth of the martensitic phase, leading to enhanced tensile strength but reduced elongation [160,161]. Implantable

medical devices, such as stents, bone plates, and artificial joints, are most commonly fabricated from the austenitic 316 SS alloy containing 2% to 3% molybdenum (Mo). However, 316L SS cannot promote new tissue growth. To address this shortcoming, a combination of this material with hydroxyapatite (HAp) has been attempted to fabricate bioactive composite implants by using the SLM method [162]. One of the major drawbacks of SS alloys for implant materials is the localized corrosion effect that causes 24% of implant failures [163]. In terms of corrosion resistance, particularly pitting resistance in fluoride-containing environments such as in the human body, 317L SS alloy with 3% to 4% Mo is better than 316L [164]. In addition to the modification of chemical composition, to improve the corrosion resistance of SS, surface modification, coating, or surface texture modification at the nanoscale can be adopted [2].

5.1.1.3 Cobalt-based alloys

Orthopedic implants are commonly fabricated from Co-Cr alloys, containing Co, Cr, Ni, and Mo. Co-based alloys have better biocompatibility, abrasion and corrosion resistance, and mechanical strength, in comparison with SS [1,2]. The high cooling rate of the SLM process can create CoCr alloy implants with higher yield strengths since it results in finer and more irregular columnar dendritic microstructures [165]. Co-Cr-Mo and Co-Ni-Cr-Mo are the two basic types of Co-Cr alloys in biomedical applications. The Co-Cr-Mo alloys have been used for dental implants and artificial joints, while the Co-Ni-Cr-Mo alloys have been used for heavy load-bearing joints. It is worth mentioning that Co-based alloys release positively charged metal ions, as they bond to the proteins and cells in the human body, and biocorrosion is one of their major problems [1,2,166–171].

5.1.1.4 Magnesium and Mg-based alloys

Many medical devices and degradable implants, namely bone screws, cardiovascular stents, and bone fixation devices can be made of biodegradable Mg and its alloys. Pure Mg has a density of 1.74 g/cm^3 being quite similar to that of natural bone with a value of 1.8 to 2.1 g/cm^3. Mg has an elastic modulus of 45 GPa, similar to that of cortical bone, and can inhibit the stress-shielding effect, but its application in the human body is yet limited due to its quick degradation that is higher than 300 μm/year under the in vitro condition due to rapid corrosion [1,2]. The elastic moduli and yield strengths of Mg-based alloys are strongly related to their chemical compositions and can be

improved through appropriate alloying. The yield strength of the SLM bulk WE43 [168] magnesium alloy reaches a value of 296.3 MPa.

Mg could be a suitable material for bone implants if the corrosion and biodegradation rate (>300 μm/year) can be controlled. Increasing the surface area or alloying Mg with Zn, Ca, Si, and Sr can help with controlling the biodegradation rate of pure Mg. Another challenge in using Mg alloys for bioimplants is the release of hydrogen into the human body while Mg is being corroded [1,2,172–176]. Furthermore, one of the most important features in AM of Mg is the extremely inflammable characteristic of Mg that has to be taken into consideration in setting up the operating condition for SLM [172]. The low boiling temperature of Mg is another consideration in choosing SLM process parameters.

5.1.1.5 Zinc and Zn-based alloys

Zn-based alloys have the most appropriate degradation rates in a range of 20 to 300 μm/year in vitro and good biocompatibility, which makes them the potential candidates for bioimplants [177,178]. Zn-based materials are mainly manufactured by the SLM process that has a narrow process window due to the low evaporation temperature of Zn [179,180]. As a result, highly porous materials were often obtained from suboptimal SLM process parameters. In addition, the low strength of Zn has limited its biomedical application. Alloying has been used to adjust the stiffness and yield strength of zinc simultaneously. For instance, by comparing Zn-Mg alloys (1%, 2%, 3%, and 4% Mg) manufactured by the SLM method with the pure zinc counterpart, it has been found that the elastic moduli and yield strengths of the SLM manufactured Zn-Mg alloys have increased significantly [181].

5.1.1.6 Iron and Fe-based alloys

Iron and its alloys are another type of biomaterials that are biodegradable and can be used for bone implants. However, their biodegradation rates are very low (less than 50 μm/year) in vitro [182]. These materials have a low hemolysis ratio and excellent anticoagulant properties. Compared to Mg and its alloys, Fe-based materials do not release hydrogen during biodegradation. In addition, they have better mechanical properties than Mg-based alloys. However, pure Fe has an elastic modulus of 211.4 GPa, which is much higher than that of pure Mg and 316L SS that have the values of 41 GPa and 190 GPa, respectively. In order to reduce the magnetic susceptibility of pure Fe and enhance its degradation rate, Fe is alloyed with a large amount of Mn, carbon (C), Si, and Pd elements [1,2].

5.1.2 Shape-memory alloys

Shape memory behavior is defined as the ability of the material to recover its initial shape by an external stimulus, such as exposure to a high temperature after being deformed. Shape memory alloys (SMAs) are promising candidates for biomedical applications, thanks to their good biocompatibility, good corrosion resistance, and high ductility. SMAs have been widely used in surgical tools, cardiovascular devices, orthopedic implants, and orthodontic wires [19,183].

Nitinol consisting of 50% Ni and 50% Ti is the most common type of SMAs and recovers its initial shape by heat-stimulated phase transformation between the martensite and austenite phases [184]. The elastic modulus of austenitic NiTi is equal to 48 GPa, which is remarkably lower than that of Ti. Moreover, NiTi can exhibit shape memory behavior for large strains up to 8% and recover its initial shape. It can withstand large strains while keeping the stress unchanged [185,186]. Considering these characteristics, nitinol is best suited for biomedical applications, e.g., surgical guide, orthodontic wires, stents, and staples for bone fracture repair [185,187,188].

A special application of almost equiatomic Ni-Ti alloy lattice structures has been found for bioimplants and microelectromechanical systems (BioMEMs) since they show a distinctive combination of thermal and mechanical shape memories, superelasticity, biocompatibility, and high corrosion resistance [184,189]. However, Ni has been found to be a highly allergenic element and may cause allergies in biomedical applications [190,191]. Therefore, in order to put this effect aside while maintaining the biocompatibility, alternative alloys, such as TiNbX (X can be Zr, Hf, or Ta), with an approximate 4.2% elastic strain have been proposed. In addition, surface modification techniques have been applied to NiTi and other SMAs to reduce Ni release and to improve their functionality. The magnetron sputtering method, for example, has been used to create carbon nitride, diamond-like carbon, or titanium nitride film in order to inhibit Ni release and improve tribological performance [192].

A number of challenges have been encountered in the manufacturing of nitinol alloy implants with complex porous shapes, considering the fact that they have low printability and high reactivity and the fact that their phase transformation temperatures and mechanical properties are strongly dependent on their exact chemical composition and microstructure which are highly sensitive to SLM process parameters [193,194]. Attempts to use AM techniques, particularly SLM as a laser-based PBF process, have been made to address the challenges in fabricating Ni-Ti SMAs [194,195].

SMA engineering designs that were previously unfeasible or exceedingly demanding using conventional fabrication technologies have shown to be realizable. In terms of the mechanical properties of AM Ni-Ti SMA implants in comparison with those of the conventionally manufactured ones, e.g., cast counterparts [185], they have exhibited similar mechanical properties. With the achievements of shape complexity and equivalent mechanical properties, the laser-based PBF technique has shown the capability to be used to manufacture Ni-Ti SMA lattice structures for a variety of biomedical applications [195–198].

5.1.3 Superalloys

Superalloys are a special group of alloys, mostly Co-, Fe-, and Ni-based alloys, which exhibit unusual and superior properties, particularly resistance against surface degradation at high temperatures. Superelasticity is one of the examples of the superior properties of some superalloys, which means that these materials are able to recover large deformations. Superelasticity is a result of mechanical deformations that cause phase transformations. For instance, Inconel superalloys such as Inconel 100, 625, 718, and 825 are a class of Ni-based alloys that are appropriate for high-temperature applications in industries such as aerospace and automobile to make use of their superior mechanical properties, together with their high creep and oxidation resistances. Thanks to the advent of the laser-based PBF processes, lattice structures with complex geometries can be made of the Inconel superalloys that are great candidates for applications in critical components and implants whose low weight and enhanced mechanical properties are of particular importance. Moreover, the Ni-based superalloys can show enhanced elongation in the vertical direction, due to the formation of columnar grains without or with γ and γ' eutectic at grain boundaries in their microstructures during the AM process, depending on the process parameters employed [199]. However, the subsequent HIP process can change the SLM columnar grains into equiaxed grains as well as mechanical performance [196–198]. Ti-based superalloys, such as titanium-molybdenum-hafnium, are suited for applications as medical implants, such as dental implants, intraosseous implants, heart valves, artificial hearts, ventricular muscle devices, bone clips, etc. [200]. The molybdenum-rhenium superalloy (Mo: 52.5% and Re: 47.5%) is a new superalloy for medical implants, as it combines high strength, ductility, durability, and biological safety, which are unmatched by other alloys [201]. SLM for such alloys to fabricate unique porous implants is yet to be explored.

5.1.4 In-situ alloying and synthesized composites

One of the advantages of AM techniques, particularly the SLM process, over the other conventional manufacturing methods is the ability to place selected materials at desired locations within the structure, which would lead to broadening the limits of complex geometry designs. The process of mixing several feedstock materials with diverse compositions is called in-situ alloying. During the SLM process, materials of different compositions are fed into the melt pool simultaneously, resulting in customized properties and functionalities from these mixtures [10].

The biofunctionalized Cu-containing Ti alloys and the SLM in-situ Ti-26Nb alloy [202] are just two examples of in-situ alloying for biomedical applications. In-situ AlSi12 alloy formation from elemental metal powders during anchorless SLM [203] has been realized with diminished residual stresses generated during the SLM process.

Generally, the aim of both in-situ alloying and, in most cases, adding ceramic reinforcing particles to a metal matrix to form a composite material is to accomplish optimized mechanical properties of the processed material, in addition to biological functionalities. To give an idea, the hardness, stiffness, and strength of the reinforcing component can be added to the intrinsic properties and thermal/electrical conductivity of the metallic matrix through the rule of mixtures. The reinforcing materials can be added to the feedstock through either ex-situ or in-situ methods. The ball milling process and mixing the alloying elements with the metal matrix are examples of ex-situ and in-situ methods, respectively. One of the most important features that have to be considered is the interactions between the matrix and the alloying elements with the ex-situ elements. Accordingly, the SLM process parameters, particularly laser power, should be properly adjusted to ensure the complete melting of the feedstock to achieve the maximum interactions between the metal matrix and the alloying elements. However, it has to be mentioned that fabricating a perfect and defect-free composite lattice structure is not an easy process, since several additional factors, such as weak interface bonding, uncompleted reactions, inhomogeneous dispersion of added particles, and interfacial cracks, would affect the quality of the manufactured structure and have to be controlled. The Ti-TiB porous composite is an example of in-situ composite formation that results from the in-situ reaction of TiB_2 reinforcing particles with the Ti matrix [204].

It has already been reported that the SLM process is capable of producing various metal matrix composites. This capability together with the ability to produce lattice structures has presented a great opportunity to the biomedical

industry to produce lattice or nonlattice structures based on purpose-designed functionally graded composite materials, or functionally graded lattice structures with gradients in chemical composition. For example, metal-ceramic composites combining partially stabilized zirconium dioxide with stainless steel are the most widely used materials in prosthesis and bipolar scissors [203,204].

6. Mechanical properties

AM materials are commonly subjected to tension, compression, fracture toughness, hardness, fatigue, and creep tests for characterizing their mechanical properties. Test specimens are prepared according to the standards, such as ASTM E8 or other comparable standards [205]. The results of these tests give information about the mechanical properties, including elastic modulus, yield strength, ultimate tensile/compressive strength, strain at failure, hardness, facture toughness, fatigue resistance, and creep resistance of AM materials. For SLM biomaterials, quasistatic compressive properties and fatigue behavior are of particular importance and they are affected by a variety of factors, including the characteristics of feedstock materials, SLM process parameters, implant design, and other factors, such as the build direction, the position of the implant within the building envelope, and the isotropic or anisotropic microstructures [119,206]. For comparison purposes, the building direction has to be reported along with the mechanical properties of AM structures [92]. A minimum number of unit cells per lattice structure is required in order to develop an authentic relationship between the "effective" mechanical properties of the lattice structure and the design of repeating unit cells (e.g., a minimum of 10-unit cells per lattice structure have been proposed in ISO 13314).

In the studies on the factors that influence the mechanical properties of solid and lattice AM materials, the chemical composition and microstructure together with crystallographic orientation are the most important ones. Furthermore, laser power, scanning speed, and the quality and characteristics of the power can also greatly influence the mechanical properties of SLM materials [42,81,92,119]. Functionally graded porous structures have unique mechanical properties that are strongly location-dependent; typically, overall elastic moduli and energy absorption capacities are enhanced in comparison to those of the uniform structures. If SLM process parameters are properly chosen, the AM process can lead to materials with mechanical properties equal to or even better than those of the materials fabricated

by using conventional methods. It is however important to note that AM materials can have lower ductility since they undergo high heating and cooling rates that cause the formation of micropores, inclusions, and non-equilibrium phases in their microstructures and the presence of residual stresses [92,119]. Moisture, oxygen, and nitrogen concentrations in feedstock materials, particularly in titanium and Ti-based alloy feedstock materials, can strongly affect the mechanical properties of AM products [207].

6.1 Quasi-static mechanical properties

Geometrical characteristics of lattice structures define their mechanical properties, including yield strength and elastic modulus through a power-law relationship $E = a\rho^b$, where a and b are geometry-dependent coefficients and ρ is the relative density (Fig. 8A and B) [206,209–212]. For stretch-dominated unit cells, for instance, the value of b is close to 1, and for bending-dominated ones, it is close to 2.

The factors that could cause differences between computationally predicted mechanical properties and the ones that are predicted by the power-law relationship are (i) the presence of residual stresses that have been generated during the SLM process [213,214], (ii) the deviations in the exact geometry of struts, and (iii) the presence of unmolten powder particles on the surface of struts, which leads to an overestimation of the relative density by applying Archimedes' technique [215,216].

Although the mechanical properties of struts can be normalized with regard to those of the bulk materials that struts are made of, the material type and microporosity in struts (Fig. 5C) can cause remarkable changes in the normalized values of elastic modulus and yield stress, as found out in a number of recent studies [217].

Diversity in postyield behavior has been observed in different metals due to their diverse plastic deformation behaviors; for example, in the lattice structure, a change in the bulk material might affect the plateau stress and densification behavior of struts at the start of their self-contact [217]. However, for AM lattice structures, the geometrical design has a much more remarkable effect on the normalized values of the quasistatic mechanical properties than the type of the material [68,217].

In AM lattice structures, the type of unit cell can influence the macroscale failure mechanisms of biomaterials under monotonic mechanical loading, while their microscale failure mechanism is independent of the geometrical design [129,212,218]. In the comparison of failure mechanism

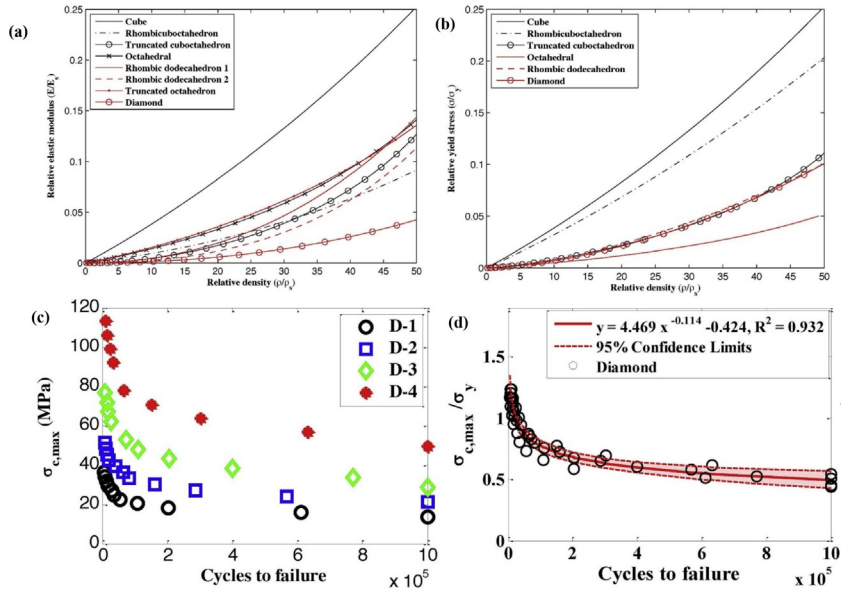

Fig. 8 The analytically predicted topology-property relationships for various beam-based lattice structures. Despite the exactly the same relative density, the (A) elastic modulus, and (B) yield strength might vary for these lattice structures [208]. The absolute S-N curves of CoCr AM lattice structures based on (C) diamond unit cells that increases with the relative density. However, (D) the S-N curve normalized with respect to the yield stress of the lattice structure is less dependent on the relative density. *((C, D) are reprinted from S.M. Ahmadi, et al., Fatigue performance of additively manufactured meta-biomaterials: the effects of topology and material type, Acta Biomater. 65 (2018) 292–304, https://doi.org/10.1016/j.actbio.2017.11.014. Copyright (2022), with permission from Elsevier.)*

between stretch-dominated and bending-dominated unit cells, stretch-dominated ones tend to fail layer-by-layer and the entire rows collapse when they are subjected to axial loading inasmuch as the struts and joints are too stiff to bend [212,219]. By contrast, in bending-dominated unit cells, the whole structure tends to collapse at once at 45° shearing bands, since they can easily rotate at their joints while they are subjected to macroscopical loads [105,218]. Another failure mechanism of unit cells that is related to the local buckling of individual struts leads to the overall failure of AM lattice structures and more brittle mechanical properties [218,219].

The typical stress-strain curves of bending-dominated and stretch-dominated lattice structures have some distinct differences. Linear elastic behavior is typically observed in a bending-dominated cellular structure

until the end of the elastic region where yield, buckle, or fracture initiates in the walls or edges of unit cells. Then, the integrity of the lattice structure is compromised around the plateau stress, σ_{pl},and densification strain, ε_d. By contrast, higher strength and elastic modulus typically occur in a stretch-dominated lattice structure and it undergoes postyield softening. In the case of biodegradable metals and alloys, the mechanical properties of AM lattice structures deteriorate along with the biodegradation process. The yield stress is much more affected by biodegradation than the elastic modulus [169,217].

6.2 Fatigue properties

Fatigue test is a cyclic test for characterizing the behavior of a biomaterial under cyclic loading. AM porous orthopedic implants are aimed to perform in bone-mimicking applications and the physical activities of the human body apply repetitive loads to orthopedic implants, which could cause fatigue failure of these materials. It is therefore important to conduct fatigue tests on them [193,220–224]. The main parameters that have to be defined in the fatigue tests are the loading frequency, maximum stress, minimum stress, and stress ratio (i.e., the ratio of minimum stress to maximum stress) [72,122,223,225–227]. It is worth noting that for determining the fatigue strength of metallic specimens with and without notch in the fatigue regime where the strains are predominately elastic, both upon initial loading and throughout the test, the ASTM E466 standard is used [226].

Load-controlled fatigue tests at a constant stress amplitude and variable stress ratio (in most cases −1 or 0.1) are the commonly performed fatigue tests of AM materials. Although the tension and bending fatigue test modes are quite sequential, compression-compression loading mode is the most preferred one in the fatigue tests of porous AM materials for biomedical applications [193,220–224]. Depending on the topological design of lattice structures, some of the struts of AM porous biomaterials can go through bending or stretching while they are subjected to compression loading. Therefore, this might develop tensile stresses in the struts of porous materials, which would act as the main source of microcrack initiation and propagation.

At the end of the fatigue tests, the results of different stress levels that have been tested are plotted in a curve called the S-N curve that presents the number of cycles to failure of each tested specimen. Fig. 8C presents an example of an S-N curve of diamond unit cell for CoCr. The endurance limit or fatigue strength is another output of this test that refers to the stress, at which the specimen fails and cannot withstand more loading cycles [227].

The fatigue behavior of AM materials can be influenced by many factors, such as residual stresses, surface roughness, and geometrical parameters such as relative density, and unit cell type [217,220,221,227]. Moreover, defects generated during the SLM process can reduce the fatigue life; for example, unmolten particles adhered to the surfaces of SLM materials could act as stress concentration points and cause premature failure of 3D-printed biomaterials. Additionally, as porosity increases, the fatigue life of lattice structures tends to decrease. Besides, as the fatigue life of AM porous structures is dependent on the plasticity of the crack tips that control the initiation and propagation of cracks, the low cycle and high cycle regions would have different fatigue life values [72].

Calculating the normalized S-N curve of a lattice structure by dividing the stress levels by the plateau or yield stress is one of the approaches that are used for removing the influences of the quasistatic mechanical properties from the dynamic effects (Fig. 8D). It has been found that in determining the fatigue life of a lattice structure the material type is more important than the topological design, particularly in the high cycle regime. The fatigue strengths of most AM lattice structures are in the range between 20% and 60% of their yield strengths, depending on their geometrical design and material type [72,220,221].

It has been reported that there is a large overlap in the S-N curve of lattice structures that have been made from the same material type and unit cell, and their S-N curves are almost the same for the implants with various porosities and thus they are not so much affected by the amount of porosity. Thanks to this valuable finding, a single normalized S-N curve can be used for evaluating the fatigue behavior of lattice structures with different amounts of porosity and there is no need to conduct separate time-consuming fatigue tests for every specimen. It has indeed been observed that the normalized S-N curves of Ti-6Al-4V lattice structures as well as those of some other alloys that have the same type of unit cell but different relative densities all fall into one curve [221]. Additionally, in favor of the idea of conducting fewer fatigue tests, it is worth noting that the fatigue crack propagation and fatigue life of AM materials can also be predicted by applying computational approaches.

In the case of studying the effect of the geometrical design of AM lattice structures, e.g., the type of the unit cell, on the fatigue life, the amplitudes of tensile stresses that are experienced in struts under compression-compression loading are determined by the geometrical design [220,228]. Fatigue resistance is enhanced in sheet-based lattice structures, as compared to that of strut-based ones for two reasons [33]. First, the former is not as sensitive

to defects and irregularities that have been formed in the AM implants during the AM process, as strut-based lattices. Second, there is no point of stress concentration in sheet-based lattice structures, since they have continuous unit cells. Continuous redistribution of stresses has been found in functionally graded lattice structures due to their inhomogeneous microstructural arrangements [129].

The tension-tension and tension-compression fatigue modes have also been studied for AM lattice structures. The results have shown that there is a decrease in the fatigue life of lattice structures in the tension-tension loading mode, as compared to the compression-compression one. By contrast, the tension-compression mode leads to enhanced fatigue life, as the number of struts which experience tensile stresses is smaller than that of struts under tension in the tension-tension and compression-compression modes [128,229].

Some of the post-AM treatments can increase the fatigue life and strength of AM lattice structures. For example, for SLM Ti-6Al-4V lattice structures, the use of HIP and surface treatments, such as sandblasting, can increase the fatigue life, after they have been applied individually or in combination with each other [124]. The HIP process can increase the fatigue limit by changing the microstructure of Ti-6Al-4V to a more ductile combination of the α and β phases and close up micropores that have been formed inside specimens during the SLM process while sandblasting can introduce compressive stresses onto the surfaces of specimens and struts of lattice structures and smoothen the surfaces of specimens. As a combined result, the ductility of pure Ti is enhanced and superelasticity of β-type Ti alloys is developed, which leads to the increases in the fatigue strengths of AM lattice structures [124,230].

The fatigue fracture surface and failure mode of porous specimens can be observed and studied by using optical deformation-tracking techniques, such as digital image correlation (DIC). These techniques can be used to confirm whether the fatigue life predictions by computational models are valid. For example, the SLM Ti-6Al-4V lattice structures based on diamond unit cells have been investigated by using the DIC technique to study the effect of stress ratio applied in the fatigue tests on the local deformation of these structures [124].

7. Conclusion and future directions

It has been demonstrated that reliable and appropriate AM lattice structures for biomedical applications can be manufactured by considering

various factors, namely geometrical design, material type, feedstock material characteristics, in-situ alloying, process parameters, and post-AM treatments. The mechanical and physical properties of lattice structure are foremost determined by their geometrical design.

In recent years, the progress in the 3D printing technology, process design and control, and selection of smart materials has led to a novel manufacturing method, namely, 4D printing, that creates 3D-printed structures being able to change their functions and configurations dynamically over time. This change can be triggered by an environmental stimulus, such as mechanical stress, temperature, light, magnetic resonance, gas pressure, pH level and so forth [229]. Apart from the choice of external stimuli, the design of 3D-printed structures plays an important role in achieving desired shapes over time. Origami and kirigami are two typical examples of shape-morphing assemblies that can be used in fabricating 4D-printed biomedical devices [230].

4D-printed medical devices may have numerous applications in the area of biomedical engineering. Examples of their applications are stent insertion [231] and drug delivery systems [232] with shape-morphing ability in the dynamic environment of the human body [233]. Another important parameter affecting the design and performance of 4D-printed medical devices is the type of stimulus-responsive smart materials. NiTi SMAs manufactured by using the SLM method are one type of potential smart metallic biomaterials that can be turned into 4D-printed biomedical devices to take advantage of their martensitic transformation that occurs with changing temperature [234]. Mechanical robustness, ductility, and resolution are some critical aspects of shape-morphing materials that must be further investigated in order to broaden their applications in the field of biomedical engineering [2,235,236].

Moreover, in order to expand the applications of 4D-printed smart structures, it is of great importance to develop the materials that can respond to more than one stimulus in different environments. This will equip these materials with multiple functionalities while they are interacting with surrounding environments [2,237].

Besides materials with programmable responses to external stimuli, mechanical metabiomaterials are another innovative category of advanced engineered materials that have recently been emerged. Their microarchitectural design features enable them to have not only high structure-related properties (e.g., low-weight-high-strength) but also high mass transport-related properties (e.g., permeability and diffusivity) [238]. In pursuit of 4D-printed high-performance smart materials, the multiphysics

theories and computational modeling are both needed to explore tailor-made properties and functionalities.

The growing interest in AM lattice structures for tissue engineering and other biomedical engineering applications have made it essential to study different SLM process parameters (e.g., laser power and scanning speed), and post-AM treatments, including mechanical surface treatments, chemical treatments, heat treatments, and HIP on their mechanical and physical properties that are negatively affected by unwanted microstructural defects at macro- and microscales. Despite the great efforts that have been made to improve the quality of SLM products, the SLM process itself is still an active field of study for the researchers to find out optimized process parameters and more importantly cost-effective methods of process optimization in order to minimize defects and ensure the quality, reproducibility, and properties of AM biomaterials, particularly fatigue properties. For example, in the case of disordered lattices, further investigations are needed to understand their fatigue behavior by conducting tests under different loading modes, namely compression-tension, tension-tension, bending, and torsion, considering the actual loading condition during the intended use.

The other recently emerged application of the AM technology concerns its intrinsic potential for manufacturing multiple materials. The AM of multimaterials enables the tailoring of materials to meet the local functional requirements for orthopedic implants by providing varied mechanical properties and characteristics perfectly matching the native tissue. Some examples of these new functionalities are controlled biodegradation and implementation of functionally graded materials for better mechanical integrity of the bone implant with the adjacent tissue [239].

In addition, artificial intelligence including deep learning and machine learning algorithms can be used as an alternative to the trial-and-error method for the development of porous biomaterials by predicting the complex relationships between chemical composition, process parameters, the microstructure of processed materials, mechanical properties, and the geometry of AM metallic materials. Clearly, only when such relationships are well established can the quality of AM implants and reproducibility be really ensured.

References

[1] Y. Li, H. Jahr, J. Zhou, A.A. Zadpoor, Additively manufactured biodegradable porous metals, Acta Biomater. 115 (2020) 29–50, https://doi.org/10.1016/j.actbio.2020.08.018.

[2] G. Liu, et al., Development of bioimplants with 2D, 3D, and 4D additive manufacturing materials, Engineering 6 (11) (2020) 1232–1243, https://doi.org/10.1016/j.eng.2020.04.015.
[3] N. Sezer, Z. Evis, M. Koç, Additive manufacturing of biodegradable magnesium implants and scaffolds: review of the recent advances and research trends, J. Magnes. Alloys 9 (2) (2021) 392–415, https://doi.org/10.1016/j.jma.2020.09.014.
[4] M. Mohammadi Zerankeshi, R. Bakhshi, R. Alizadeh, Polymer/metal composite 3D porous bone tissue engineering scaffolds fabricated by additive manufacturing techniques: a review, Bioprinting 25 (2022), e00191, https://doi.org/10.1016/j.bprint.2022.e00191.
[5] R. Kumar, M. Kumar, J.S. Chohan, The role of additive manufacturing for biomedical applications: a critical review, J. Manuf. Process. 64 (2021) 828–850, https://doi.org/10.1016/j.jmapro.2021.02.022 (Elsevier Ltd).
[6] J.S. Cuellar, G. Smit, D. Plettenburg, A. Zadpoor, Additive manufacturing of non-assembly mechanisms, Addit. Manuf. 21 (February) (2018) 150–158, https://doi.org/10.1016/j.addma.2018.02.004.
[7] A. Nouri, A.R. Shirvan, Y. Li, C. Wen, Additive manufacturing of metallic and polymeric load-bearing biomaterials using laser powder bed fusion: a review, J. Mater. Sci. Technol. (2021), https://doi.org/10.1016/j.jmst.2021.03.058.
[8] H. Lee, C.H.J. Lim, M.J. Low, N. Tham, V.M. Murukeshan, Y.J. Kim, Lasers in additive manufacturing: a review, Int. J. Precis. Eng. Manuf. Green Technol. 4 (3) (2017) 307–322, https://doi.org/10.1007/s40684-017-0037-7.
[9] B. Dutta, F.H.S. Froes, The additive manufacturing (AM) of titanium alloys, Met. Powder Rep. 72 (2) (2017) 96–106, https://doi.org/10.1016/j.mprp.2016.12.062.
[10] D. Bourell, et al., Materials for additive manufacturing, CIRP Ann. 66 (2) (2017) 659–681, https://doi.org/10.1016/J.CIRP.2017.05.009.
[11] A. Rifai, S. Houshyar, K. Fox, Progress towards 3D-printing diamond for medical implants: a review, Ann. 3D Print. Med. 1 (2021), 100002, https://doi.org/10.1016/j.stlm.2020.100002.
[12] P.K. Gokuldoss, S. Kolla, J. Eckert, J. Stampfl, Additive manufacturing processes: selective laser melting, electron beam melting and binder jetting-selection guidelines, Materials (2017), https://doi.org/10.3390/ma10060672 (MDPI AG).
[13] A.D. Sebastian Bremen, W. Meiners, Selective laser melting a manufacturing technology for the future? Laser Tech. J. 9 (2) (2012) 33–38.
[14] L.E. Murr, et al., Metal fabrication by additive manufacturing using laser and electron beam melting technologies, J. Mater. Sci. Technol. 28 (1) (2012) 1–14, https://doi.org/10.1016/S1005-0302(12)60016-4.
[15] S.M. Ahmadi, et al., Effects of laser processing parameters on the mechanical properties, topology, and microstructure of additively manufactured porous metallic biomaterials: a vector-based approach, Mater. Des. 134 (2017) 234–243, https://doi.org/10.1016/J.MATDES.2017.08.046.
[16] J. Zielinski, S. Vervoort, H.-W. Mindt, M. Megahed, Influence of powder bed characteristics on material quality in additive manufacturing, BHM Berg- Hüttenmänn. Monatsh. 162 (5) (2017) 192–198, https://doi.org/10.1007/s00501-017-0592-9.
[17] R. McCann, et al., In-situ sensing, process monitoring and machine control in laser powder bed fusion: a review, Addit. Manuf. 45 (November 2020) (2021), https://doi.org/10.1016/j.addma.2021.102058.
[18] R. Kawalkar, H.K. Dubey, S.P. Lokhande, A review for advancements in standardization for additive manufacturing, Mater. Today Proc. (2021), https://doi.org/10.1016/j.matpr.2021.09.333.
[19] X. Wang, et al., Topological design and additive manufacturing of porous metals for bone scaffolds and orthopaedic implants: a review, Biomaterials 83 (2016) 127–141, https://doi.org/10.1016/J.BIOMATERIALS.2016.01.012.

[20] S.J.P. Callens, R.J.C. Uyttendaele, L.E. Fratila-Apachitei, A.A. Zadpoor, Substrate curvature as a cue to guide spatiotemporal cell and tissue organization, Biomaterials 232 (2020), 119739, https://doi.org/10.1016/j.biomaterials.2019.119739 (Elsevier).
[21] C.P. de Jonge, H.M.A. Kolken, A.A. Zadpoor, Non-auxetic mechanical metamaterials, Materials 12 (4) (2019), https://doi.org/10.3390/ma12040635.
[22] A.A. Zadpoor, Design for additive bio-manufacturing: from patient-specific medical devices to rationally designed meta-biomaterials, Int. J. Mol. Sci. 18 (2017) 1607, https://doi.org/10.3390/ijms18081607.
[23] T. Maconachie, et al., SLM lattice structures: properties, performance, applications and challenges, Mater. Des. 183 (2019), 108137, https://doi.org/10.1016/j.matdes.2019.108137.
[24] I. Maskery, N.T. Aboulkhair, A.O. Aremu, C.J. Tuck, I.A. Ashcroft, Compressive failure modes and energy absorption in additively manufactured double gyroid lattices, Addit. Manuf. 16 (2017) 24–29, https://doi.org/10.1016/J.ADDMA.2017.04.003.
[25] M. Mirzaali, H. Pahlavani, A. Zadpoor, Auxeticity and stiffness of random networks: lessons for the rational design of 3D printed mechanical metamaterials, Appl. Phys. Lett. 115 (2) (2019) 021901, https://doi.org/10.1063/1.5096590.
[26] V.S. Deshpande, M.F. Ashby, N.A. Fleck, Foam topology: bending versus stretching dominated architectures, Acta Mater. 49 (6) (2001) 1035–1040, https://doi.org/10.1016/S1359-6454(00)00379-7.
[27] S.C. Kapfer, S.T. Hyde, K. Mecke, C.H. Arns, G.E. Schröder-Turk, Minimal surface scaffold designs for tissue engineering, Biomaterials 32 (29) (2011) 6875–6882, https://doi.org/10.1016/J.BIOMATERIALS.2011.06.012.
[28] D.J. Yoo, Porous scaffold design using the distance field and triply periodic minimal surface models, Biomaterials 32 (31) (2011) 7741–7754, https://doi.org/10.1016/j.biomaterials.2011.07.019.
[29] D.J. Yoo, Computer-aided porous scaffold design for tissue engineering using triply periodic minimal surfaces, Int. J. Precis. Eng. Manuf. 12 (1) (2011) 61–71, https://doi.org/10.1007/s12541-011-0008-9.
[30] M. Mirzaali, F. Bobbert, Y. Li, A. Zadpoor, Additive manufacturing of metals using powder bed-based technologies, in: Additive Manufacturing, Taylor & Francis Group, 2019, pp. 93–145.
[31] G.H. Loh, E. Pei, D. Harrison, M.D. Monzón, An overview of functionally graded additive manufacturing, Addit. Manuf. 23 (2018) 34–44, https://doi.org/10.1016/J.ADDMA.2018.06.023.
[32] A.A. Zadpoor, Bone tissue regeneration: the role of scaffold geometry, Biomater. Sci. 3 (2) (2015) 231–245, https://doi.org/10.1039/c4bm00291a.
[33] F.S.L. Bobbert, et al., Additively manufactured metallic porous biomaterials based on minimal surfaces: a unique combination of topological, mechanical, and mass transport properties, Acta Biomater. 53 (2017) 572–584, https://doi.org/10.1016/j.actbio.2017.02.024.
[34] S.Y. Choy, C.N. Sun, K.F. Leong, J. Wei, Compressive properties of functionally graded lattice structures manufactured by selective laser melting, Mater. Des. 131 (2017) 112–120, https://doi.org/10.1016/J.MATDES.2017.06.006.
[35] Z. Hashin, S. Shtrikman, A variational approach to the theory of the elastic behaviour of multiphase materials, J. Mech. Phys. Solids 11 (2) (1963) 127–140, https://doi.org/10.1016/0022-5096(63)90060-7.
[36] J. Berger, H. Wadley, R. McMeeking, Mechanical metamaterials at the theoretical limit of isotropic elastic stiffness, Nature 543 (2017) 533–537, https://doi.org/10.1038/nature21075.
[37] M.P. Bendsoe, O. Sigmund, Topology Optimization: Theory, Methods, and Applications, Springer Science & Business Media, 2013.

[38] A. Bensoussan, J.L. Lions, G. Papanicolaou, Asymptotic Analysis for Periodic Structures, American Mathematical Soc., 2011.
[39] O. Sigmund, S. Torquato, Design of materials with extreme thermal expansion using a three-phase topology optimization method, J. Mech. Phys. Solids 45 (6) (1997) 1037–1067, https://doi.org/10.1016/S0022-5096(96)00114-7.
[40] A.A. Zadpoor, G. Campoli, H. Weinans, Neural network prediction of load from the morphology of trabecular bone, Appl. Math. Model. 37 (7) (2013) 5260–5276, https://doi.org/10.1016/j.apm.2012.10.049.
[41] A.A. Zadpoor, Open forward and inverse problems in theoretical modeling of bone tissue adaptation, J. Mech. Behav. Biomed. Mater. 27 (2013) 249–261, https://doi.org/10.1016/j.jmbbm.2013.05.017.
[42] A.A. Zadpoor, Mechanics of additively manufactured biomaterials, J. Mech. Behav. Biomed. Mater. 70 (2017) 1–6, https://doi.org/10.1016/j.jmbbm.2017.03.018 (Elsevier).
[43] M. Fraldi, L. Esposito, G. Perrella, A. Cutolo, S.C. Cowin, Topological optimization in hip prosthesis design, Biomech. Model. Mechanobiol. 9 (4) (2010) 389–402, https://doi.org/10.1007/s10237-009-0183-0.
[44] H.G. Chuah, I. Abd Rahim, M.I. Yusof, Topology optimisation of spinal interbody cage for reducing stress shielding effect, Comput. Methods Biomech. Biomed. Eng. 13 (3) (2010) 319–326, https://doi.org/10.1080/10255840903208189.
[45] C.Y. Lin, N. Kikuchi, S.J. Hollister, A novel method for biomaterial scaffold internal architecture design to match bone elastic properties with desired porosity, J. Biomech. 37 (5) (2004) 623–636, https://doi.org/10.1016/j.jbiomech.2003.09.029.
[46] S.J. Hollister, R.D. Maddox, J.M. Taboas, Optimal design and fabrication of scaffolds to mimic tissue properties and satisfy biological constraints, Biomaterials 23 (20) (2002) 4095–4103, https://doi.org/10.1016/S0142-9612(02)00148-5.
[47] S. Yuan, C.K. Chua, K. Zhou, 3D-printed mechanical metamaterials with high energy absorption, Adv. Mater. Technol. 4 (3) (2019) 1–9, https://doi.org/10.1002/admt.201800419.
[48] J.K. Guest, J.H. Prévost, Optimizing multifunctional materials: design of microstructures for maximized stiffness and fluid permeability, Int. J. Solids Struct. 43 (22–23) (2006) 7028–7047, https://doi.org/10.1016/j.ijsolstr.2006.03.001.
[49] G. Ryan, A. Pandit, D.P. Apatsidis, Fabrication methods of porous metals for use in orthopaedic applications, Biomaterials 27 (13) (2006) 2651–2670, https://doi.org/10.1016/J.BIOMATERIALS.2005.12.002.
[50] Y.M. Xie, G.P. Steven, A simple evolutionary procedure for structural optimization, Comput. Struct. 49 (5) (1993) 885–896, https://doi.org/10.1016/0045-7949(93)90035-C.
[51] M. Zhou, G.I.N. Rozvany, The COC algorithm, part II: topological, geometrical and generalized shape optimization, Comput. Methods Appl. Mech. Eng. 89 (1–3) (1991) 309–336, https://doi.org/10.1016/0045-7825(91)90046-9.
[52] M.P. Bendsoe, Optimal shape design as a material distribution problem, Struct. Optim. 1 (4) (1989) 193–202, https://doi.org/10.1007/BF01650949.
[53] X. Huang, Y.M. Xie, Bi-directional evolutionary topology optimization of continuum structures with one or multiple materials, Comput. Mech. 43 (3) (2009) 393–401, https://doi.org/10.1007/s00466-008-0312-0.
[54] M.Y. Wang, X. Wang, D. Guo, A level set method for structural topology optimization, Comput. Methods Appl. Mech. Eng. 192 (1–2) (2003) 227–246, https://doi.org/10.1016/S0045-7825(02)00559-5.
[55] D.T. Blacker, M. Aguilo, B. Clark, J. Robbins, S. Owens, T. Voth, PLATO Platinum Topology Optimization, 2015.

[56] M. Langelaar, Combined optimization of part topology, support structure layout and build orientation for additive manufacturing, Struct. Multidiscip. Optim. 57 (5) (2018) 1985–2004, https://doi.org/10.1007/s00158-017-1877-z.
[57] T.A. Krol, M.F. Zaeh, C. Seidel, Optimization of supports in metal-based additive manufacturing by means of finite element models, in: 23rd Annu. Int. Solid Free. Fabr. Symp. - An Addit. Manuf. Conf. SFF 2012, 2012, pp. 707–718.
[58] A. Ataee, Y. Li, D. Fraser, G. Song, C. Wen, Anisotropic Ti-6Al-4V gyroid scaffolds manufactured by electron beam melting (EBM) for bone implant applications, Mater. Des. 137 (2018) 345–354, https://doi.org/10.1016/J.MATDES.2017.10.040.
[59] M.I. Mohammed, I. Gibson, Design of three-dimensional, triply periodic unit cell scaffold structures for additive manufacturing, J. Mech. Des. 140 (7) (2018), 071701.
[60] A. Yánez, A. Cuadrado, O. Martel, H. Afonso, D. Monopoli, Gyroid porous titanium structures: a versatile solution to be used as scaffolds in bone defect reconstruction, Mater. Des. 140 (2018) 21–29, https://doi.org/10.1016/j.matdes.2017.11.050.
[61] E.L. Doubrovski, E.Y. Tsai, D. Dikovsky, J.M.P. Geraedts, H. Herr, N. Oxman, Voxel-based fabrication through material property mapping: a design method for bitmap printing, Comput. Aided Des. 60 (2015) 3–13, https://doi.org/10.1016/j.cad.2014.05.010.
[62] B.S. Bucklen, W.A. Wettergreen, E. Yuksel, M.A.K. Liebschner, Bone-derived CAD library for assembly of scaffolds in computer-aided tissue engineering, Virtual Phys. Prototyp. 3 (1) (2008) 13–23, https://doi.org/10.1080/17452750801911352.
[63] S. Bose, S. Vahabzadeh, A. Bandyopadhyay, Bone tissue engineering using 3D printing, Mater. Today 16 (12) (2013) 496–504, https://doi.org/10.1016/j.mattod.2013.11.017 (Elsevier).
[64] J. Parthasarathy, 3D modeling, custom implants and its future perspectives in craniofacial surgery, Ann. Maxillofac. Surg. 4 (1) (2014) 9, https://doi.org/10.4103/2231-0746.133065.
[65] S.J. Hollister, R.A. Levy, T.M. Chu, J.W. Halloran, S.E. Feinberg, An image-based approach for designing and manufacturing craniofacial scaffolds, Int. J. Oral Maxillofac. Surg. 29 (1) (2000) 67–71, https://doi.org/10.1034/j.1399-0020.2000.290115.x.
[66] M. van Eijnatten, R. van Dijk, J. Dobbe, G. Streekstra, J. Koivisto, J. Wolff, CT image segmentation methods for bone used in medical additive manufacturing, Med. Eng. Phys. 51 (2018) 6–16, https://doi.org/10.1016/j.medengphy.2017.10.008 (Elsevier).
[67] M. Ding, X. Lin, W. Liu, Three-dimensional morphometric properties of rod- and plate-like trabeculae in adolescent cancellous bone, J. Orthop. Transl. 12 (2018) 26–35, https://doi.org/10.1016/j.jot.2017.10.001.
[68] A.A. Zadpoor, Mechanical performance of additively manufactured meta-biomaterials, Acta Biomater. 85 (2019) 41–59, https://doi.org/10.1016/j.actbio.2018.12.038.
[69] A.A. Zadpoor, Frontiers of additively manufactured metallic materials, Materials 11 (9) (2018), https://doi.org/10.3390/ma11091566.
[70] H.M.A.A. Kolken, A.A. Zadpoor, Auxetic mechanical metamaterials, RSC Adv. 7 (9) (2017) 5111–5129, https://doi.org/10.1039/c6ra27333e.
[71] V. Karageorgiou, D. Kaplan, Porosity of 3D biomaterial scaffolds and osteogenesis, Biomaterials 26 (27) (2005) 5474–5491, https://doi.org/10.1016/j.biomaterials.2005.02.002.
[72] S.M. Ahmadi, et al., Fatigue performance of additively manufactured meta-biomaterials: the effects of topology and material type, Acta Biomater. 65 (2018) 292–304, https://doi.org/10.1016/j.actbio.2017.11.014.

[73] C.M. Bidan, F.M. Wang, J.W.C. Dunlop, A three-dimensional model for tissue deposition on complex surfaces, Comput. Methods Biomech. Biomed. Eng. 16 (10) (2013) 1056–1070, https://doi.org/10.1080/10255842.2013.774384.
[74] J. Beuth, et al., Process mapping for qualification across multiple direct metal additive manufacturing processes, in: 24th Int. SFF Symp. - An Addit. Manuf. Conf. SFF 2013, 2013, pp. 655–665.
[75] J. Beuth, N. Klingbeil, The role of process variables in laser-based direct metal solid freeform fabrication, JOM 53 (9) (2001) 36–39, https://doi.org/10.1007/s11837-001-0067-y.
[76] J. Gockel, J. Beuth, Understanding Ti-6Al-4V microstructure control in additive manufacturing via process maps, in: 24th Int. SFF Symp. - An Addit. Manuf. Conf. SFF 2013, 2013, pp. 666–674.
[77] M. Elsayed, M. Ghazy, Y. Youssef, K. Essa, Optimization of SLM process parameters for Ti6Al4V medical implants, Rapid Prototyp. J. 25 (3) (2019) 433–447, https://doi.org/10.1108/RPJ-05-2018-0112.
[78] T. Brajlih, B. Valentan, J. Balic, I. Drstvensek, Speed and accuracy evaluation of additive manufacturing machines, Rapid Prototyp. J. 17 (1) (2011) 64–75, https://doi.org/10.1108/13552541111098644.
[79] B.N. Turner, S.A. Gold, A review of melt extrusion additive manufacturing processes: II. Materials, dimensional accuracy, and surface roughness, Rapid Prototyp. J. 21 (3) (2015) 250–261, https://doi.org/10.1108/RPJ-02-2013-0017.
[80] A. El Elmi, D. Melancon, M. Asgari, L. Liu, D. Pasini, Experimental and numerical investigation of selective laser melting–induced defects in Ti–6Al–4V octet truss lattice material: the role of material microstructure and morphological variations, J. Mater. Res. 35 (15) (2020) 1900–1912, https://doi.org/10.1557/jmr.2020.75.
[81] H. Bikas, P. Stavropoulos, G. Chryssolouris, Additive manufacturing methods and modeling approaches: a critical review, Int. J. Adv. Manuf. Technol. 83 (1–4) (2016) 389–405, https://doi.org/10.1007/s00170-015-7576-2.
[82] G. Strano, L. Hao, R.M. Everson, K.E. Evans, Surface roughness analysis, modelling and prediction in selective laser melting, J. Mater. Process. Technol. 213 (4) (2013) 589–597, https://doi.org/10.1016/J.JMATPROTEC.2012.11.011.
[83] B. Nagarajan, Z. Hu, X. Song, W. Zhai, J. Wei, Development of Micro selective laser melting: the state of the art and future perspectives, Engineering 5 (4) (2019) 702–720, https://doi.org/10.1016/j.eng.2019.07.002 (Elsevier Ltd).
[84] R.R. Dehoff, et al., Case study: additive manufacturing of aerospace brackets, Adv. Mater. Process. 171 (3) (2013) 19–22.
[85] E. Lyczkowska, P. Szymczyk, B. Dybała, E. Chlebus, Chemical polishing of scaffolds made of Ti–6Al–7Nb alloy by additive manufacturing, Arch. Civ. Mech. Eng. 14 (4) (2014) 586–594, https://doi.org/10.1016/J.ACME.2014.03.001.
[86] M. Entezarian, F. Allaire, P. Tsantrizos, R.A.L. Drew, Plasma atomization: a new process for the production of fine, spherical powders, JOM 48 (6) (1996) 53–55, https://doi.org/10.1007/BF03222969.
[87] H.K. Rafi, N.V. Karthik, H. Gong, T.L. Starr, B.E. Stucker, Microstructures and mechanical properties of Ti6Al4V parts fabricated by selective laser melting and electron beam melting, J. Mater. Eng. Perform. 22 (12) (2013) 3872–3883, https://doi.org/10.1007/s11665-013-0658-0.
[88] A.J. Pinkerton, L. Li, Direct additive laser manufacturing using gas- and water-atomised H13 tool steel powders, Int. J. Adv. Manuf. Technol. 25 (5–6) (2005) 471–479, https://doi.org/10.1007/s00170-003-1844-2.
[89] H.P. Tang, M. Qian, N. Liu, X.Z. Zhang, G.Y. Yang, J. Wang, Effect of powder reuse times on additive manufacturing of Ti-6Al-4V by selective Electron beam melting, JOM 67 (3) (2015) 555–563, https://doi.org/10.1007/s11837-015-1300-4.

[90] D. Gu, Y. Shen, Balling phenomena in direct laser sintering of stainless steel powder: metallurgical mechanisms and control methods, Mater. Des. 30 (8) (2009) 2903–2910, https://doi.org/10.1016/J.MATDES.2009.01.013.
[91] J.P. Kruth, L. Froyen, J. Van Vaerenbergh, P. Mercelis, M. Rombouts, B. Lauwers, Selective laser melting of iron-based powder, J. Mater. Process. Technol. 149 (1–3) (2004) 616–622, https://doi.org/10.1016/j.jmatprotec.2003.11.051.
[92] H.J. Niu, I.T.H. Chang, Instability of scan tracks of selective laser sintering of high speed steel powder, Scr. Mater. 41 (11) (1999) 1229–1234, https://doi.org/10.1016/S1359-6462(99)00276-6.
[93] W.E. Frazier, Metal additive manufacturing: a review, J. Mater. Eng. Perform. 23 (6) (2014) 1917–1928.
[94] T. Vilaro, C. Colin, J.D. Bartout, As-fabricated and heat-treated microstructures of the Ti-6Al-4V alloy processed by selective laser melting, Metall. Mater. Trans. A Phys. Metall. Mater. Sci. 42 (10) (2011) 3190–3199, https://doi.org/10.1007/s11661-011-0731-y.
[95] A.B. Spierings, G. Levy, Comparison of density of stainless steel 316L parts produced with selective laser melting using different powder grades, in: Proceedings of the 20th Solid Freeform Fabrication Symposium, Austin, Texas, 2009, pp. 324–353.
[96] S.L. Sing, F.E. Wiria, W.Y. Yeong, Selective laser melting of lattice structures: a statistical approach to manufacturability and mechanical behavior, Robot. Comput. Integr. Manuf. 49 (2018) 170–180, https://doi.org/10.1016/j.rcim.2017.06.006.
[97] H. Salem, L.N. Carter, M.M. Attallah, H.G. Salem, Influence of processing parameters on internal porosity and types of defects formed in Ti6Al4V lattice structure fabricated by selective laser melting, Mater. Sci. Eng. A 767 (2019), 138387, https://doi.org/10.1016/j.msea.2019.138387.
[98] C. Cosma, J. Kessler, A. Gebhardt, I. Campbell, N. Balc, Improving the mechanical strength of dental applications and lattice structures SLM processed, Materials 13 (4) (2020), https://doi.org/10.3390/ma13040905.
[99] X. Zhang, C.J. Yocom, B. Mao, Y. Liao, Microstructure evolution during selective laser melting of metallic materials: a review, J. Laser Appl. 31 (3) (2019), 031201, https://doi.org/10.2351/1.5085206.
[100] J. Gockel, J. Beuth, K. Taminger, Integrated control of solidification microstructure and melt pool dimensions in electron beam wire feed additive manufacturing of ti-6al-4v, Addit. Manuf. 1 (2014) 119–126, https://doi.org/10.1016/j.addma.2014.09.004.
[101] A.R. Nassar, J.S. Keist, E.W. Reutzel, T.J. Spurgeon, Intra-layer closed-loop control of build plan during directed energy additive manufacturing of Ti-6Al-4V, Addit. Manuf. 6 (2015) 39–52, https://doi.org/10.1016/j.addma.2015.03.005.
[102] A. Saboori, G. Donato, B. Sara, F. Paolo, L. Mariangela, An overview of additive manufacturing of titanium components by directed energy deposition: microstructure and mechanical properties, Appl. Sci. (2017), https://doi.org/10.3390/app7090883.
[103] X. Tan, et al., Graded microstructure and mechanical properties of additive manufactured Ti-6Al-4V via electron beam melting, Acta Mater. 97 (2015) 1–16,- https://doi.org/10.1016/j.actamat.2015.06.036.
[104] J. Alcisto, et al., Tensile properties and microstructures of laser-formed Ti-6Al-4V, J. Mater. Eng. Perform. 20 (2) (2011) 203–212, https://doi.org/10.1007/s11665-010-9670-9.
[105] L.E. Murr, et al., Microstructural architecture, microstructures, and mechanical properties for a nickel-base superalloy fabricated by electron beam melting, Metall. Mater. Trans. A Phys. Metall. Mater. Sci. 42 (11) (2011) 3491–3508, https://doi.org/10.1007/s11661-011-0748-2.

[106] B.E. Carroll, T.A. Palmer, A.M. Beese, Anisotropic tensile behavior of Ti-6Al-4V components fabricated with directed energy deposition additive manufacturing, Acta Mater. 87 (2015) 309–320, https://doi.org/10.1016/j.actamat.2014.12.054.
[107] C. Körner, H. Helmer, A. Bauereiß, R.F. Singer, Tailoring the grain structure of IN718 during selective electron beam melting, MATEC Web Conf. 14 (2014), https://doi.org/10.1051/matecconf/20141408001.
[108] L. Thijs, M.L. Montero Sistiaga, R. Wauthle, Q. Xie, J.P. Kruth, J. Van Humbeeck, Strong morphological and crystallographic texture and resulting yield strength anisotropy in selective laser melted tantalum, Acta Mater. 61 (12) (2013) 4657–4668, https://doi.org/10.1016/j.actamat.2013.04.036.
[109] S. Bontha, N.W. Klingbeil, P.A. Kobryn, H.L. Fraser, Thermal process maps for predicting solidification microstructure in laser fabrication of thin-wall structures, J. Mater. Process. Technol. 178 (1–3) (2006) 135–142, https://doi.org/10.1016/j.jmatprotec.2006.03.155.
[110] P.C. Collins, D.A. Brice, P. Samimi, I. Ghamarian, H.L. Fraser, Microstructural control of additively manufactured metallic materials, Annu. Rev. Mater. Res. 46 (2016) 63–91, https://doi.org/10.1146/annurev-matsci-070115-031816.
[111] I. Campbell, D. Bourell, I. Gibson, Additive manufacturing: rapid prototyping comes of age, Rapid Prototyp. J. 18 (4) (2012) 255–258, https://doi.org/10.1108/13552541211231563.
[112] Q. Wang, et al., Effect of Nb content on microstructure, property and in vitro apatite-forming capability of Ti-Nb alloys fabricated via selective laser melting, Mater. Des. 126 (2017) 268–277, https://doi.org/10.1016/j.matdes.2017.04.026.
[113] H.P. Tang, J. Wang, M. Qian, Porous titanium structures and applications, in: Titanium Powder Metallurgy: Science, Technology and Applications, Butterworth-Heinemann, 2015, pp. 533–554.
[114] D.S. Shim, J.Y. Seo, H.S. Yoon, K.Y. Lee, W.J. Oh, Additive manufacturing of porous metals using laser melting of Ti6Al4V powder with a foaming agent, Mater. Res. Express 5 (8) (2018), 086518, https://doi.org/10.1088/2053-1591/aad117.
[115] P. Mercelis, J.P. Kruth, Residual stresses in selective laser sintering and selective laser melting, Rapid Prototyp. J. 12 (5) (2006) 254–265, https://doi.org/10.1108/13552540610707013.
[116] K. Dai, L. Shaw, Distortion minimization of laser-processed components through control of laser scanning patterns, Rapid Prototyp. J. 8 (5) (2002) 270–276, https://doi.org/10.1108/13552540210451732.
[117] P. Rangaswamy, et al., Residual stresses in LENS® components using neutron diffraction and contour method, Mater. Sci. Eng. A 399 (1–2) (2005) 72–83, https://doi.org/10.1016/j.msea.2005.02.019.
[118] R.J. Moat, A.J. Pinkerton, L. Li, P.J. Withers, M. Preuss, Residual stresses in laser direct metal deposited Waspaloy, Mater. Sci. Eng. A 528 (6) (2011) 2288–2298, https://doi.org/10.1016/j.msea.2010.12.010.
[119] E. Brandl, D. Greitemeier, Microstructure of additive layer manufactured Ti–6Al–4V after exceptional post heat treatments, Mater. Lett. 81 (2012) 84–87, https://doi.org/10.1016/J.MATLET.2012.04.116.
[120] J.J. Lewandowski, M. Seifi, Metal additive manufacturing: a review of mechanical properties, Annu. Rev. Mater. Res. 46 (2016) 151–186, https://doi.org/10.1146/annurev-matsci-070115-032024.
[121] B. Song, S. Dong, Q. Liu, H. Liao, C. Coddet, Vacuum heat treatment of iron parts produced by selective laser melting: microstructure, residual stress and tensile behavior, Mater. Des. 54 (2014) 727–733, https://doi.org/10.1016/J.MATDES.2013.08.085.
[122] B. Vrancken, L. Thijs, J.P. Kruth, J. Van Humbeeck, Heat treatment of Ti6Al4V produced by selective laser melting: microstructure and mechanical properties, J. Alloys Compd. 541 (2012) 177–185, https://doi.org/10.1016/J.JALLCOM.2012.07.022.

[123] L. Yang, et al., Compression–compression fatigue behaviour of gyroid-type triply periodic minimal surface porous structures fabricated by selective laser melting, Acta Mater. 181 (2019) 49–66, https://doi.org/10.1016/j.actamat.2019.09.042.
[124] K.S. Chan, M. Koike, R.L. Mason, T. Okabe, Fatigue life of titanium alloys fabricated by additive layer manufacturing techniques for dental implants, Metall. Mater. Trans. A Phys. Metall. Mater. Sci. 44 (2) (2013) 1010–1022, https://doi.org/10.1007/s11661-012-1470-4.
[125] L.N. Carter, M.M. Attallah, R.C. Reed, Laser powder bed fabrication of nickel-base superalloys: Influence of parameters; characterisation, quantification and mitigation of cracking, in: Proc. Int. Symp. Superalloys, 2012, pp. 577–586, https://doi.org/10.7449/2012/superalloys_2012_577_586.
[126] S.M. Ahmadi, et al., From microstructural design to surface engineering: a tailored approach for improving fatigue life of additively manufactured meta-biomaterials, Acta Biomater. 83 (2019) 153–166, https://doi.org/10.1016/J.ACTBIO.2018.10.043.
[127] S. Tammas-Williams, P.J. Withers, I. Todd, P.B. Prangnell, The effectiveness of hot isostatic pressing for closing porosity in titanium parts manufactured by selective Electron beam melting, Metall. Mater. Trans. A Phys. Metall. Mater. Sci. 47 (5) (2016) 1939–1946, https://doi.org/10.1007/s11661-016-3429-3.
[128] B. Van Hooreweder, J.P. Kruth, Advanced fatigue analysis of metal lattice structures produced by selective laser melting, CIRP Ann. Manuf. Technol. 66 (1) (2017) 221–224, https://doi.org/10.1016/j.cirp.2017.04.130.
[129] M.W. Wu, P.H. Lai, The positive effect of hot isostatic pressing on improving the anisotropies of bending and impact properties in selective laser melted Ti-6Al-4V alloy, Mater. Sci. Eng. A 658 (2016) 429–438, https://doi.org/10.1016/j.msea.2016.02.023.
[130] M. Dallago, et al., Fatigue and biological properties of Ti-6Al-4V ELI cellular structures with variously arranged cubic cells made by selective laser melting, J. Mech. Behav. Biomed. Mater. 78 (2018) 381–394, https://doi.org/10.1016/j.jmbbm.2017.11.044.
[131] A. Cutolo, B. Neirinck, K. Lietaert, C. de Formanoir, B. Van Hooreweder, Influence of layer thickness and post-process treatments on the fatigue properties of CoCr scaffolds produced by laser powder bed fusion, Addit. Manuf. 23 (2018) 498–504, https://doi.org/10.1016/j.addma.2018.07.008.
[132] G. Kasperovich, J. Hausmann, Improvement of fatigue resistance and ductility of TiAl6V4 processed by selective laser melting, J. Mater. Process. Technol. 220 (2015) 202–214, https://doi.org/10.1016/j.jmatprotec.2015.01.025.
[133] M.W. Wu, J.K. Chen, B.H. Lin, P.H. Chiang, Improved fatigue endurance ratio of additive manufactured Ti-6Al-4V lattice by hot isostatic pressing, Mater. Des. 134 (2017) 163–170, https://doi.org/10.1016/j.matdes.2017.08.048.
[134] S. Amin Yavari, et al., Layer by layer coating for bio-functionalization of additively manufactured meta-biomaterials, Addit. Manuf. 32 (2020) 100991, https://doi.org/10.1016/j.addma.2019.100991.
[135] I.A.J. Van Hengel, et al., Self-defending additively manufactured bone implants bearing silver and copper nanoparticles, J. Mater. Chem. B 8 (8) (2020) 1589–1602, https://doi.org/10.1039/c9tb02434d.
[136] S.M. Ahmadi, et al., Mechanical behavior of regular open-cell porous biomaterials made of diamond lattice unit cells, J. Mech. Behav. Biomed. Mater. 34 (2014) 106–115, https://doi.org/10.1016/J.JMBBM.2014.02.003.
[137] K.C. Nune, R.D.K. Misra, X. Gai, S.J. Li, Y.L. Hao, Surface nanotopography-induced favorable modulation of bioactivity and osteoconductive potential of

anodized 3D printed Ti-6Al-4V alloy mesh structure, J. Biomater. Appl. 32 (8) (2018) 1032–1048, https://doi.org/10.1177/0885328217748860.
[138] M.J. Mirzaali, A.H. de la Nava, D. Gunashekar, M. Nouri-Goushki, E.L. Doubrovski, A.A. Zadpoor, Fracture behavior of bio-inspired functionally graded soft-hard composites made by multi-material 3D printing: the case of colinear cracks, Materials 12 (7) (2019), https://doi.org/10.3390/ma12172735.
[139] I.C. Brie, et al., Comparative in vitro study regarding the biocompatibility of titanium-base composites infiltrated with hydroxyapatite or silicatitanate, J. Biol. Eng. 8 (1) (2014) 1–19, https://doi.org/10.1186/1754-1611-8-14.
[140] S.F.S. Shirazi, et al., A review on powder-based additive manufacturing for tissue engineering: selective laser sintering and inkjet 3D printing, Sci. Technol. Adv. Mater. 16 (3) (2015), https://doi.org/10.1088/1468-6996/16/3/033502.
[141] Z. Gorgin Karaji, R. Hedayati, B. Pouran, I. Apachitei, A.A. Zadpoor, Effects of plasma electrolytic oxidation process on the mechanical properties of additively manufactured porous biomaterials, Mater. Sci. Eng. C 76 (2017) 406–416, https://doi.org/10.1016/J.MSEC.2017.03.079.
[142] P. Heinl, L. Müller, C. Körner, R.F. Singer, F.A. Müller, Cellular Ti-6Al-4V structures with interconnected macro porosity for bone implants fabricated by selective electron beam melting, Acta Biomater. 4 (5) (2008) 1536–1544, https://doi.org/10.1016/j.actbio.2008.03.013.
[143] X. Li, et al., Evaluation of biological properties of electron beam melted Ti6Al4V implant with biomimetic coating in vitro and in vivo, PLoS One 7 (12) (2012), https://doi.org/10.1371/journal.pone.0052049.
[144] S. Amin Yavari, et al., Effects of bio-functionalizing surface treatments on the mechanical behavior of open porous titanium biomaterials, J. Mech. Behav. Biomed. Mater. 36 (2014) 109–119, https://doi.org/10.1016/j.jmbbm.2014.04.010.
[145] G. Pyka, et al., Surface modification of Ti6Al4V open porous structures produced by additive manufacturing, Adv. Eng. Mater. 14 (6) (2012) 363–370, https://doi.org/10.1002/adem.201100344.
[146] S. Amin Yavari, R. Wauthle, A.J. Böttger, J. Schrooten, H. Weinans, A.A. Zadpoor, Crystal structure and nanotopographical features on the surface of heat-treated and anodized porous titanium biomaterials produced using selective laser melting, Appl. Surf. Sci. 290 (2014) 287–294, https://doi.org/10.1016/J.APSUSC.2013.11.069.
[147] M.A.-H. Gepreel, M. Niinomi, Biocompatibility of Ti-alloys for long-term implantation, J. Mech. Behav. Biomed. Mater. 20 (2013) 407–415, https://doi.org/10.1016/J.JMBBM.2012.11.014.
[148] M. Long, H.J. Rack, Titanium alloys in total joint replacement – a materials science perspective, Biomaterials 19 (18) (1998) 1621–1639, https://doi.org/10.1016/S0142-9612(97)00146-4 (Elsevier).
[149] L. Thijs, F. Verhaeghe, T. Craeghs, J. Van Humbeeck, J.P. Kruth, A study of the microstructural evolution during selective laser melting of Ti-6Al-4V, Acta Mater. 58 (9) (2010) 3303–3312, https://doi.org/10.1016/j.actamat.2010.02.004.
[150] J. Yu, M. Rombouts, G. Maes, F. Motmans, Material properties of Ti6Al4 v parts produced by laser metal deposition, Phys. Procedia 39 (2012) 416–424, https://doi.org/10.1016/j.phpro.2012.10.056.
[151] A.T. Sidambe, Biocompatibility of advanced manufactured titanium implants-a review, Materials 7 (12) (2014) 8168–8188, https://doi.org/10.3390/ma7128168.
[152] S.S. Sidhu, H. Singh, M.A.H. Gepreel, A review on alloy design, biological response, and strengthening of β-titanium alloys as biomaterials, Mater. Sci. Eng. C 121 (2021), 111661, https://doi.org/10.1016/j.msec.2020.111661.
[153] J.A. Helsen, Y. Missirlis, Biomaterials: A Tantalus Experience, Springer Science & Business Media, 2010.

[154] A. Barbas, A.S. Bonnet, P. Lipinski, R. Pesci, G. Dubois, Development and mechanical characterization of porous titanium bone substitutes, J. Mech. Behav. Biomed. Mater. 9 (2012) 34–44, https://doi.org/10.1016/j.jmbbm.2012.01.008.
[155] M. De Wild, et al., Bone regeneration by the osteoconductivity of porous titanium implants manufactured by selective laser melting: a histological and micro computed tomography study in the rabbit, Tissue Eng. A 19 (23–24) (2013) 2645–2654, https://doi.org/10.1089/ten.tea.2012.0753.
[156] X. Liu, P.K. Chu, C. Ding, Surface modification of titanium, titanium alloys, and related materials for biomedical applications, Mater. Sci. Eng. R. Rep. 47 (3–4) (2004) 49–121, https://doi.org/10.1016/j.mser.2004.11.001 (Elsevier).
[157] R. Wauthle, et al., Revival of pure titanium for dynamically loaded porous implants using additive manufacturing, Mater. Sci. Eng. C 54 (2015) 94–100, https://doi.org/10.1016/J.MSEC.2015.05.001.
[158] D.M. Brunette, P. Tengvall, M. Textor, P. Thomsen, Titanium in Medicine: Material Science, Surface Science, Engineering, Biological Responses and Medical Applications, Springer Science & Business Media, 2012.
[159] A.L. Jardini, et al., Customised titanium implant fabricated in additive manufacturing for craniomaxillofacial surgery: this paper discusses the design and fabrication of a metallic implant for the reconstruction of a large cranial defect, Virtual Phys. Prototyp. 9 (2) (2014) 115–125, https://doi.org/10.1080/17452759.2014.900857.
[160] L.E. Murr, et al., Microstructures and properties of 17-4 PH stainless steel fabricated by selective laser melting, J. Mater. Res. Technol. 1 (3) (2012) 167–177, https://doi.org/10.1016/S2238-7854(12)70029-7.
[161] J. Suryawanshi, K.G. Prashanth, U. Ramamurty, Mechanical behavior of selective laser melted 316L stainless steel, Mater. Sci. Eng. A 696 (2017) 113–121, https://doi.org/10.1016/j.msea.2017.04.058.
[162] L. Hao, S. Dadbakhsh, O. Seaman, M. Felstead, Selective laser melting of a stainless steel and hydroxyapatite composite for load-bearing implant development, J. Mater. Process. Technol. 209 (17) (2009) 5793–5801, https://doi.org/10.1016/j.jmatprotec.2009.06.012.
[163] M.J.K. Lodhi, K.M. Deen, M.C. Greenlee-Wacker, W. Haider, Additively manufactured 316L stainless steel with improved corrosion resistance and biological response for biomedical applications, Addit. Manuf. 27 (2019) 8–19, https://doi.org/10.1016/j.addma.2019.02.005.
[164] N. Eliaz, Corrosion of metallic biomaterials: a review, Materials 12 (3) (2019) 407, https://doi.org/10.3390/ma12030407 (MDPI AG).
[165] L.E. Murr, et al., Microstructure and mechanical properties of open-cellular biomaterials prototypes for total knee replacement implants fabricated by electron beam melting, J. Mech. Behav. Biomed. Mater. 4 (7) (2011) 1396–1411, https://doi.org/10.1016/j.jmbbm.2011.05.010.
[166] B. Vandenbroucke, J.P. Kruth, Selective laser melting of biocompatible metals for rapid manufacturing of medical parts, in: 17th Solid Free. Fabr. Symp. SFF 2006, 2006, pp. 148–159.
[167] N. Xiang, X.Z. Xin, J. Chen, B. Wei, Metal-ceramic bond strength of Co-Cr alloy fabricated by selective laser melting, J. Dent. 40 (6) (2012) 453–457, https://doi.org/10.1016/j.jdent.2012.02.006.
[168] X.Z. Xin, N. Xiang, J. Chen, B. Wei, In vitro biocompatibility of Co-Cr alloy fabricated by selective laser melting or traditional casting techniques, Mater. Lett. 88 (2012) 101–103, https://doi.org/10.1016/j.matlet.2012.08.032.
[169] F.A. España, V.K. Balla, S. Bose, A. Bandyopadhyay, Design and fabrication of CoCrMo alloy based novel structures for load bearing implants using laser engineered

net shaping, Mater. Sci. Eng. C 30 (1) (2010) 50–57, https://doi.org/10.1016/j.msec.2009.08.006.
[170] L.E. Murr, S.M. Gaytan, E. Martinez, F. Medina, R.B. Wicker, Next generation orthopaedic implants by additive manufacturing using electron beam melting, Int. J. Biomater. 2012 (2012) 14, https://doi.org/10.1155/2012/245727.
[171] T. Koutsoukis, S. Zinelis, G. Eliades, K. Al-Wazzan, M. Al Rifaiy, Y.S. Al Jabbari, Selective laser melting technique of Co-Cr dental alloys: a review of structure and properties and comparative analysis with other available techniques, J. Prosthodont. 24 (4) (2015) 303–312, https://doi.org/10.1111/jopr.12268.
[172] Y. Li, et al., Additively manufactured biodegradable porous magnesium, Acta Biomater. 67 (2018) 378–392, https://doi.org/10.1016/J.ACTBIO.2017.12.008.
[173] R. Erbel, et al., Temporary scaffolding of coronary arteries with bioabsorbable magnesium stents: a prospective, non-randomised multicentre trial, Lancet 369 (9576) (2007) 1869–1875, https://doi.org/10.1016/S0140-6736(07)60853-8.
[174] H. Windhagen, et al., Biodegradable magnesium-based screw clinically equivalent to titanium screw in hallux valgus surgery: short term results of the first prospective, randomized, controlled clinical pilot stud, Biomed. Eng. Online 12 (1) (2013), https://doi.org/10.1186/1475-925X-12-62.
[175] Y.F. Zheng, X.N. Gu, F. Witte, Biodegradable metals, Mater. Sci. Eng. R. Rep. 77 (2014) 1–34, https://doi.org/10.1016/J.MSER.2014.01.001.
[176] L. Yuan, S. Ding, C. Wen, Additive manufacturing technology for porous metal implant applications and triple minimal surface structures: a review, Bioact. Mater. 4 (1) (2019) 56–70, https://doi.org/10.1016/j.bioactmat.2018.12.003.
[177] P. Wen, L. Jauer, M. Voshage, Y. Chen, R. Poprawe, J.H. Schleifenbaum, Densification behavior of pure Zn metal parts produced by selective laser melting for manufacturing biodegradable implants, J. Mater. Process. Technol. 258 (2018) 128–137, https://doi.org/10.1016/j.jmatprotec.2018.03.007.
[178] Y. Hou, et al., Synthesis of biodegradable Zn-based scaffolds using NaCl templates: relationship between porosity, compressive properties and degradation behavior, Mater. Charact. 137 (2018) 162–169, https://doi.org/10.1016/J.MATCHAR.2018.01.033.
[179] P. Wen, et al., Laser additive manufacturing of Zn metal parts for biodegradable applications: processing, formation quality and mechanical properties, Mater. Des. 155 (2018) 36–45, https://doi.org/10.1016/j.matdes.2018.05.057.
[180] M. Montani, A.G. Demir, E. Mostaed, M. Vedani, B. Previtali, Article information: processability of pure Zn and pure Fe by SLM for biodegradable metallic implant manufacturing, Rapid Prototyp. J. (2017).
[181] Y. Li, J. Shi, H. Jahr, J. Zhou, A.A. Zadpoor, L. Wang, Improving the mechanical properties of additively manufactured Micro-architected biodegradable metals, JOM 73 (2021) 1–11.
[182] H. Li, Y. Zheng, L. Qin, Progress of biodegradable metals, Prog. Nat. Sci. Mater. Int. 24 (5) (2014) 414–422, https://doi.org/10.1016/j.pnsc.2014.08.014 (Elsevier).
[183] S. Dadbakhsh, M. Speirs, J. Van Humbeeck, J.P. Kruth, Laser additive manufacturing of bulk and porous shape-memory NiTi alloys: from processes to potential biomedical applications, MRS Bull. 41 (10) (2016) 765–774, https://doi.org/10.1557/mrs.2016.209.
[184] M.H. Elahinia, M. Hashemi, M. Tabesh, S.B. Bhaduri, Manufacturing and processing of NiTi implants: a review, Prog. Mater. Sci. 57 (5) (2012) 911–946, https://doi.org/10.1016/j.pmatsci.2011.11.001.
[185] C. Haberland, M. Elahinia, J.M. Walker, H. Meier, J. Frenzel, On the development of high quality NiTi shape memory and pseudoelastic parts by additive manufacturing,

Smart Mater. Struct. 23 (10) (2014), 104002, https://doi.org/10.1088/0964-1726/23/10/104002.
[186] N.B. Morgan, Medical shape memory alloy applications—the market and its products, Mater. Sci. Eng. A 378 (1–2) (2004) 16–23, https://doi.org/10.1016/J.MSEA.2003.10.326.
[187] Z. Gorgin Karaji, et al., Additively manufactured and surface biofunctionalized porous nitinol, ACS Appl. Mater. Interfaces 9 (2) (2016) 1293–1304, https://doi.org/10.1021/acsami.6b14026.
[188] S. Dadbakhsh, B. Vrancken, J.P. Kruth, J. Luyten, J. Van Humbeeck, Texture and anisotropy in selective laser melting of NiTi alloy, Mater. Sci. Eng. A 650 (2016) 225–232, https://doi.org/10.1016/j.msea.2015.10.032.
[189] A. Mitchell, U. Lafont, M. Hołyńska, C.J.A.M. Semprimoschnig, Additive manufacturing — a review of 4D printing and future applications, Addit. Manuf. 24 (2018) 606–626, https://doi.org/10.1016/J.ADDMA.2018.10.038.
[190] A. Biesiekierski, J. Wang, M. Abdel-Hady Gepreel, C. Wen, A new look at biomedical Ti-based shape memory alloys, Acta Biomater. 8 (5) (2012) 1661–1669, https://doi.org/10.1016/J.ACTBIO.2012.01.018.
[191] R. Köster, et al., Nickel and molybdenum contact allergies in patients with coronary in-stent restenosis, ACC Curr. J. Rev. 3 (10) (2001) 62, https://doi.org/10.1016/S0140-6736(00)03262-1.
[192] J. Wang, M. Liu, Study on the tribological properties of hard films deposited on biomedical NiTi alloy, Mater. Chem. Phys. 129 (1–2) (2011) 40–45, https://doi.org/10.1016/j.matchemphys.2011.03.051.
[193] T. Bormann, B. Müller, M. Schinhammer, A. Kessler, P. Thalmann, M. De Wild, Microstructure of selective laser melted nickel-titanium, Mater. Charact. 94 (2014) 189–202, https://doi.org/10.1016/j.matchar.2014.05.017.
[194] J. Van Humbeeck, Additive manufacturing of shape memory alloys, Shape Mem. Superelasticity 4 (2) (2018) 309–312, https://doi.org/10.1007/s40830-018-0174-z.
[195] M. Speirs, B. Van Hooreweder, J. Van Humbeeck, J.P. Kruth, Fatigue behaviour of NiTi shape memory alloy scaffolds produced by SLM, a unit cell design comparison, J. Mech. Behav. Biomed. Mater. 70 (2017) 53–59, https://doi.org/10.1016/J.JMBBM.2017.01.016.
[196] X. Wang, S. Kustov, J. Van Humbeeck, A short review on the microstructure, transformation behavior and functional properties of NiTi shape memory alloys fabricated by selective laser melting, Materials 11 (9) (2018), https://doi.org/10.3390/ma11091683.
[197] T. Habijan, et al., The biocompatibility of dense and porous nickel–titanium produced by selective laser melting, Mater. Sci. Eng. C 33 (1) (2013) 419–426, https://doi.org/10.1016/J.MSEC.2012.09.008.
[198] S. Bernard, V. Krishna Balla, S. Bose, A. Bandyopadhyay, Compression fatigue behavior of laser processed porous NiTi alloy, J. Mech. Behav. Biomed. Mater. 13 (2012) 62–68, https://doi.org/10.1016/J.JMBBM.2012.04.010.
[199] Z. Chen, et al., Anisotropy of nickel-based superalloy K418 fabricated by selective laser melting, Prog. Nat. Sci. Mater. Int. 28 (4) (2018) 496–504, https://doi.org/10.1016/j.pnsc.2018.07.001.
[200] J.A. Davidson, Titanium Molybdenum Hafnium Alloys for Medical Implants and Devices, 1997.
[201] S. Shepard, Image Courtesy of MiRus Using Advanced Materials to Make Better Implants Is Just the Starting Point for MiRus, 2019.
[202] M. Fischer, D. Joguet, G. Robin, L. Peltier, P. Laheurte, In situ elaboration of a binary Ti–26Nb alloy by selective laser melting of elemental titanium and niobium mixed

powders, Mater. Sci. Eng. C 62 (2016) 852–859, https://doi.org/10.1016/J.MSEC.2016.02.033.
[203] P. Vora, K. Mumtaz, I. Todd, N. Hopkinson, AlSi12 in-situ alloy formation and residual stress reduction using anchorless selective laser melting, Addit. Manuf. 7 (2015) 12–19, https://doi.org/10.1016/J.ADDMA.2015.06.003.
[204] L.C. Zhang, H. Attar, Selective laser melting of titanium alloys and titanium matrix composites for biomedical applications: a review, Adv. Eng. Mater. 18 (4) (2016) 463–475, https://doi.org/10.1002/adem.201500419.
[205] ASTM/ISO, ASTM52921-13 standard terminology for additive manufacturing-coordinate systems and test methodologies, in: West Conshohocken ASTM Int., 2013.
[206] M.F. Ashby, The properties of foams and lattices, Philos. Trans. R. Soc. A Math. Phys. Eng. Sci. 364 (1838) (2006) 15–30, https://doi.org/10.1098/rsta.2005.1678.
[207] B. Vrancken, S. Buls, J.-P. Kruth, J. Van Humbeeck, Preheating of selective laser melted Ti6Al4V: microstructure and mechanical properties, in: Proceedings of the 13th World Conference on Titanium, San Diego, CL, 2016, pp. 1269–1277, https://doi.org/10.1002/9781119296126.ch215. Aug. 16–20.
[208] A. Abbas Zadpoor, R. Hedayati, Review article analytical relationships for prediction of the mechanical properties of additively manufactured porous biomaterials, J. Biomed. Mater. Res. A 104 (2016) 3164–3174, https://doi.org/10.1002/jbm.a.35855.
[209] L.J. Ibson, M.F. Ashby, Cellular Solids: Structure and Properties, Cambridge University, 1999.
[210] R. Hedayati, M. Sadighi, M. Mohammadi-Aghdam, A.A. Zadpoor, Effect of mass multiple counting on the elastic properties of open-cell regular porous biomaterials, Mater. Des. 89 (2016) 9–20, https://doi.org/10.1016/j.matdes.2015.09.052.
[211] R. Hedayati, M. Sadighi, M. Mohammadi-Aghdam, A.A. Zadpoor, Mechanical properties of regular porous biomaterials made from truncated cube repeating unit cells: analytical solutions and computational models, Mater. Sci. Eng. C 60 (2016) 163–183, https://doi.org/10.1016/J.MSEC.2015.11.001.
[212] V.S. Deshpande, N.A. Fleck, M.F. Ashby, Effective properties of the octet-truss lattice material, J. Mech. Phys. Solids 49 (8) (2001) 1747–1769, https://doi.org/10.1016/S0022-5096(01)00010-2.
[213] Z. Wang, E. Denlinger, P. Michaleris, A.D. Stoica, D. Ma, A.M. Beese, Residual stress mapping in Inconel 625 fabricated through additive manufacturing: method for neutron diffraction measurements to validate thermomechanical model predictions, Mater. Des. 113 (2017) 169–177, https://doi.org/10.1016/j.matdes.2016.10.003.
[214] C. Yan, L. Hao, A. Hussein, P. Young, D. Raymont, Advanced lightweight 316L stainless steel cellular lattice structures fabricated via selective laser melting, Mater. Des. 55 (2014) 533–541, https://doi.org/10.1016/j.matdes.2013.10.027.
[215] Y. Wang, L. Zhang, S. Daynes, H. Zhang, S. Feih, M.Y. Wang, Design of graded lattice structure with optimized mesostructures for additive manufacturing, Mater. Des. 142 (2018) 114–123, https://doi.org/10.1016/j.matdes.2018.01.011.
[216] M. Yakout, M.A. Elbestawi, S.C. Veldhuis, Density and mechanical properties in selective laser melting of invar 36 and stainless steel 316L, J. Mater. Process. Technol. 266 (2019) 397–420, https://doi.org/10.1016/j.jmatprotec.2018.11.006.
[217] R. Hedayati, et al., Isolated and modulated effects of topology and material type on the mechanical properties of additively manufactured porous biomaterials, J. Mech. Behav. Biomed. Mater. 79 (2018) 254–263, https://doi.org/10.1016/J.JMBBM.2017.12.029.

[218] S.J. Li, et al., Influence of cell shape on mechanical properties of Ti-6Al-4V meshes fabricated by electron beam melting method, Acta Biomater. 10 (10) (2014) 4537–4547, https://doi.org/10.1016/j.actbio.2014.06.010.
[219] J. Kadkhodapour, et al., Failure mechanisms of additively manufactured porous biomaterials: effects of porosity and type of unit cell, J. Mech. Behav. Biomed. Mater. 50 (2015) 180–191, https://doi.org/10.1016/J.JMBBM.2015.06.012.
[220] S. Amin Yavari, et al., Relationship between unit cell type and porosity and the fatigue behavior of selective laser melted meta-biomaterials, J. Mech. Behav. Biomed. Mater. 43 (2015) 91–100, https://doi.org/10.1016/J.JMBBM.2014.12.015.
[221] S. Amin Yavari, et al., Fatigue behavior of porous biomaterials manufactured using selective laser melting, Mater. Sci. Eng. C 33 (8) (2013) 4849–4858, https://doi.org/10.1016/J.MSEC.2013.08.006.
[222] G. Campoli, M.S. Borleffs, S. Amin Yavari, R. Wauthle, H. Weinans, A.A. Zadpoor, Mechanical properties of open-cell metallic biomaterials manufactured using additive manufacturing, Mater. Des. 49 (2013) 957–965, https://doi.org/10.1016/j.matdes.2013.01.071.
[223] E. Amsterdam, G.A. Kool, High cycle fatigue of laser beam deposited Ti-6Al-4V and inconel 718, in: ICAF 2009, Bridg. Gap Between Theory Oper. Pract. - Proc. 25th Symp. Int. Comm. Aeronaut. Fatigue, May, 2009, pp. 1261–1274, https://doi.org/10.1007/978-90-481-2746-7_71.
[224] N.W. Hrabe, P. Heinl, B. Flinn, C. Körner, R.K. Bordia, Compression-compression fatigue of selective electron beam melted cellular titanium (Ti-6Al-4V), J. Biomed. Mater. Res. B Appl. Biomater. 99 B (2) (2011) 313–320, https://doi.org/10.1002/jbm.b.31901.
[225] K.D. Rekedal, D. Liu, Fatigue life of selective laser melted and hot isostatically pressed Ti-6Al-4v absent of surface machining, in: 56th AIAA/ASCE/AHS/ASC Struct. Struct. Dyn. Mater. Conf., January, 2015, pp. 1–9, https://doi.org/10.2514/6.2015-0894.
[226] A. W. I. WK49229, Guide for Orientation and Location Dependence Mechanical Properties for Metal Additive Manufacturing, Am. Soc. Test. Mater., 2015.
[227] A. Zargarian, M. Esfahanian, J. Kadkhodapour, S. Ziaei-Rad, Numerical simulation of the fatigue behavior of additive manufactured titanium porous lattice structures, Mater. Sci. Eng. C 60 (2016) 339–347, https://doi.org/10.1016/j.msec.2015.11.054.
[228] S. Zhao, S.J. Li, W.T. Hou, Y.L. Hao, R. Yang, R.D.K. Misra, The influence of cell morphology on the compressive fatigue behavior of Ti-6Al-4V meshes fabricated by electron beam melting, J. Mech. Behav. Biomed. Mater. 59 (2016) 251–264, https://doi.org/10.1016/j.jmbbm.2016.01.034.
[229] S. Tibbits, 4D printing: multi-material shape change, Archit. Des. 84 (1) (2014) 116–121, https://doi.org/10.1002/ad.1710.
[230] J.A. Faber, A.F. Arrieta, A.R. Studart, Bioinspired spring origami, Science 359 (6382) (2018) 1386–1391, https://doi.org/10.1126/science.aap7753 More.
[231] B. Rapp, Managing technowaste, Mater. Today 12 (7) (2004) 13, https://doi.org/10.1016/S1369-7021(04)00548-6.
[232] C.L. Randall, E. Gultepe, D.H. Gracias, Self-folding devices and materials for biomedical applications, Trends Biotechnol. 30 (3) (2012) 138–146, https://doi.org/10.1016/j.tibtech.2011.06.013.
[233] R.L. Truby, J.A. Lewis, Printing soft matter in three dimensions, Nature 540 (7633) (2016) 371–378, https://doi.org/10.1038/nature21003 (Nature Publishing Group).
[234] S. Dadbakhsh, M. Speirs, J.P. Kruth, J. Schrooten, J. Luyten, J. Van Humbeeck, Effect of SLM parameters on transformation temperatures of shape memory nickel titanium parts, Adv. Eng. Mater. 16 (9) (2014) 1140–1146.

[235] A. Sydney Gladman, E.A. Matsumoto, R.G. Nuzzo, L. Mahadevan, J.A. Lewis, Biomimetic 4D printing, Nat. Mater. 15 (4) (2016) 413–418, https://doi.org/10.1038/nmat4544.
[236] S.K. Saha, D. Wang, V.H. Nguyen, Y. Chang, J.S. Oakdale, S.-C. Chen, Scalable submicrometer additive manufacturing, Science 366 (6461) (2019) 105–109, https://doi.org/10.1126/science.aax8760 (Speeding).
[237] Y. Dong, J. Wang, X. Guo, S. Yang, M.O. Ozen, P. Chen, Multi-stimuliresponsive programmable biomimetic actuator, Nat. Commun. 10 (1) (2019) 1–10, https://doi.org/10.1038/s41467-019-12044-5.
[238] G. Liu, et al., Additive manufacturing of structural materials, Mater. Sci. Eng. R. Rep. 145 (2021), 100596, https://doi.org/10.1016/j.mser.2020.100596.
[239] N.E. Putra, M.J. Mirzaali, I. Apachitei, J. Zhou, A.A. Zadpoor, Multi-material additive manufacturing technologies for Ti-, Mg-, and Fe-based biomaterials for bone substitution, Acta Biomater. 109 (2020) 1–20, https://doi.org/10.1016/j.actbio.2020.03.037.